

# Structural Characterization of Many-Particle Systems on Approach to Hyperuniform States

Salvatore Torquato\*

*Department of Chemistry, Department of Physics,  
Princeton Institute for the Science and Technology of Materials,  
and Program in Applied and Computational Mathematics,  
Princeton University, Princeton, New Jersey 08544, USA*

(Dated: September 23, 2021)

The study of hyperuniform states of matter is an emerging multidisciplinary field, impinging on topics in the physical sciences, mathematics and biology. The focus of this work is the exploration of quantitative descriptors that herald when a many-particle system in  $d$ -dimensional Euclidean space  $\mathbb{R}^d$  approaches a hyperuniform state as a function of the relevant control parameter. We establish quantitative criteria to ascertain the extent of hyperuniform and nonhyperuniform distance-scaling regimes as well as the crossover point between them in terms of the “volume” coefficient  $A$  and “surface-area” coefficient  $B$  associated with the local number variance  $\sigma^2(R)$  for a spherical window of radius  $R$ . The larger the ratio  $B/A$ , the larger the hyperuniform scaling regime, which becomes of infinite extent in the limit  $B/A \rightarrow \infty$ . To complement the known direct-space representation of the coefficient  $B$  in terms of the total correlation function  $h(\mathbf{r})$ , we derive its corresponding Fourier representation in terms of the structure factor  $S(\mathbf{k})$ , which is especially useful when scattering information is available experimentally or theoretically. We also demonstrate that the free-volume theory of the pressure of equilibrium packings of identical hard spheres that approach a strictly jammed state either along the stable crystal or metastable disordered branch dictates that such end states be exactly hyperuniform. Using the ratio  $B/A$ , as well as other diagnostic measures of hyperuniformity, including the hyperuniformity index  $H$  and the direct-correlation function length scale  $\xi_c$ , we study three different exactly solvable models as a function of the relevant control parameter, either density or temperature, with end states that are perfectly hyperuniform. Specifically, we analyze equilibrium systems of hard rods and “sticky” hard-sphere systems in arbitrary space dimension  $d$  as a function of density. We also examine low-temperature excited states of many-particle systems interacting with “stealthy” long-ranged pair interactions as the temperature tends to zero, where the ground states are disordered, hyperuniform and infinitely degenerate. We demonstrate that our various diagnostic hyperuniformity measures are positively correlated with one another. The same diagnostic measures can be used to detect the degree to which imperfections in nearly hyperuniform systems cause deviations from perfect hyperuniformity. Moreover, the capacity to identify hyperuniform scaling regimes should be particularly useful in analyzing experimentally- or computationally-generated samples that are necessarily of finite size.

## I. INTRODUCTION

A hyperuniform point configuration in  $d$ -dimensional Euclidean space  $\mathbb{R}^d$  is characterized by an anomalous suppression of large-scale density fluctuations relative to those in typical disordered systems, such as liquids and structural glasses [1, 2]. More precisely, a hyperuniform point pattern is one in which the structure factor  $S(\mathbf{k}) \equiv 1 + \rho \tilde{h}(\mathbf{k})$  tends to zero as the wavenumber  $k \equiv |\mathbf{k}|$  tends to zero [1, 2], i.e.,

$$\lim_{|\mathbf{k}| \rightarrow 0} S(\mathbf{k}) = 0, \quad (1)$$

where  $\tilde{h}(\mathbf{k})$  is the Fourier transform of the total correlation function  $h(\mathbf{r}) \equiv g_2(\mathbf{r}) - 1$  and  $g_2(\mathbf{r})$  is the pair-correlation function [3]. The hyperuniformity concept generalizes the traditional notion of long-range order in many-particle systems to include all perfect crystals, perfect quasicrystals, and exotic amorphous states of matter. Disordered hyperuniform materials can have advantages over crystalline ones, such as unique or nearly optimal, direction-independent physical properties and robustness against defects [4–16].

An equivalent definition of hyperuniformity is based on the local number variance  $\sigma^2(R) \equiv \langle N(R)^2 \rangle - \langle N(R) \rangle^2$  associated with the number  $N(R)$  of points within a  $d$ -dimensional spherical observation window of radius  $R$ , where angular brackets denote an ensemble average. A point pattern in  $\mathbb{R}^d$  is hyperuniform if its variance grows in the large- $R$  limit slower than  $R^d$ . This behavior is to be contrasted with those of typical disordered systems, such as Poisson point patterns, gases and liquids, where the number variance scales like the volume  $v_1(R)$  of the observation window, which is given by

$$v_1(R) = \frac{\pi^{d/2} R^d}{\Gamma(1 + d/2)}. \quad (2)$$

Consider systems that are characterized by a structure factor with a radial power-law form in the vicinity of the origin, i.e.,

$$S(\mathbf{k}) \sim |\mathbf{k}|^\alpha \quad \text{for } |\mathbf{k}| \rightarrow 0. \quad (3)$$

For hyperuniform systems, the exponent  $\alpha$  is positive ( $\alpha > 0$ ) and its value determines three different large-

$R$  scaling behaviors of the number variance [1, 2, 17]:

$$\sigma^2(R) \sim \begin{cases} R^{d-1}, & \alpha > 1 \text{ (class I)} \\ R^{d-1} \ln R, & \alpha = 1 \text{ (class II)} \\ R^{d-\alpha}, & \alpha < 1 \text{ (class III)} \end{cases} \quad (4)$$

These scalings of  $\sigma^2(R)$  define three classes of hyperuniformity [2], with classes I and III describing the strongest and weakest forms of hyperuniformity, respectively. States of matter that belong to class I include all perfect crystals [1, 17], many perfect quasicrystals [17–19], and “randomly” perturbed crystal structures [20–23], classical disordered ground states of matter [1, 24, 25] as well as systems out of equilibrium [26, 27]. Class II hyperuniform systems include some quasicrystals [19], the positions of the prime numbers [28], and many disordered classical [26, 29–32] and quantum [33–35] states of matter. Examples of class III hyperuniform systems include classical disordered ground states [36], random organization models [37] and perfect glasses [26].

By contrast, for any nonhyperuniform system, it is shown in Appendix A that the local variance has the following large- $R$  scaling behaviors:

$$\sigma^2(R) \sim \begin{cases} R^d, & \alpha = 0^+ \text{ (typical nonhyperuniform)} \\ R^{d-\alpha}, & \alpha < 0 \text{ (anti-hyperuniform)} \end{cases} \quad (5)$$

For a “typical” nonhyperuniform system,  $S(0)$  is bounded [2]. In *anti-hyperuniform* systems,  $S(0)$  is unbounded, i.e.,

$$\lim_{|\mathbf{k}| \rightarrow 0} S(\mathbf{k}) = +\infty, \quad (6)$$

and hence are diametrically opposite to hyperuniform systems. Anti-hyperuniform systems include fractals, systems at thermal critical points (e.g., liquid-vapor and magnetic critical points) [38–42] as well as certain substitution tilings [43].

Our main concern in this paper is the exploration of quantitative descriptors that herald when a many-particle system is nearly hyperuniform or approaching a hyperuniform state, whether ordered or not. Elucidating such questions not only is expected to lead to a deeper fundamental understanding of the nature and formation of hyperuniform systems but has great practical value. For example, since hyperuniformity can endow a system with novel or optimal physical properties, it is essential to know how close the system must be to perfect hyperuniformity without significantly degrading its ideal performance. In practice, perfect hyperuniformity is never achieved due to defects that are inevitably present in any real finite-sized system [44], whether crystalline, quasicrystalline or disordered [23].

We begin by recalling pertinent previous concepts and results (Sec. II), including the fluctuation-compressibility theorem, hyperuniformity as a critical

phenomenon, a hyperuniformity length scale  $\xi_c$  and a hyperuniformity index  $H$ . The latter two quantities provide measures of nearness to hyperuniformity.

In the remainder of the paper, we obtain a variety of theoretical results to study the problem at hand. First, for a general system, we establish quantitative criteria to ascertain the extent of hyperuniform and nonhyperuniform distance-scaling regimes as well as the crossover point between them in terms of the “volume” coefficient  $A$  and “surface-area” coefficient  $B$  associated with the variance  $\sigma^2(R)$  (Sec. III). Specifically, the ratio  $B/A$  determines the crossover length scale  $R_c$ . The larger the ratio  $B/A$ , the larger the hyperuniform scaling regime, which becomes of infinite extent in the limit  $B/A \rightarrow \infty$ . This capacity to determine hyperuniform scaling regimes is expected to be particularly useful in analyzing experimentally- or computationally-generated samples that are necessarily of finite size.

Second, to complement the known direct-space representation of the coefficient  $B$  in terms of the total correlation function  $h(\mathbf{r})$  [1], we derive here its corresponding Fourier representation in terms of the structure factor  $S(\mathbf{k})$  (Sec. IV). The latter representation is particularly useful when the scattering intensity is available experimentally or if the structure factor is known analytically.

Third, we show that the free-volume theory of the pressure of equilibrium packings of identical hard spheres that approach either a strictly jammed crystal or disordered state dictates that such jammed states be perfectly hyperuniform (Sec. V). We describe why this outcome implies that such jammed states must be defect-free.

Fourth, motivated by a desire to rely on analytical rather than numerical methods, we structurally characterize three different disordered-system models as a function of the relevant control parameter, either density or temperature, with end states that are perfectly hyperuniform. These models are distinguished from most other models with hyperuniform states in that their pair correlation functions and structure factors are known exactly for all values of the control parameter in the thermodynamic limit. We purposely avoid the use of simulations of many-particle systems in finite boxes to draw conclusions, since hyperuniformity is an infinite-wavelength property. The first model that we characterize is an equilibrium system of hard rods (Sec. VI). Here the control parameter is the number density  $\rho$  (or packing fraction) and its terminal value corresponds to the jammed state that is the integer lattice. The second model studied is a certain “sticky” hard-sphere system in arbitrary space dimension  $d$  as a function of the number density (or packing fraction) (Sec. VII). The third model that we characterize are low-temperature excited states of so-called stealthy long-ranged pair interactions in  $\mathbb{R}^d$  (Sec. VIII). Here, the control parameter is the temperature  $T$  and the corresponding ground states at  $T = 0$  are disordered and degenerate.

## II. COMPRESSIBILITY, INVERTED CRITICAL POINT, GROWING LENGTH SCALE AND HYPERUNIFORMITY INDEX

In this section, we briefly review pertinent background material. This outline includes the implications of the fluctuation-compressibility theorem, hyperuniformity as a critical phenomenon, a length scale that grows on approach to a hyperuniform state, and the hyperuniformity index.

### A. Fluctuation-Compressibility Theorem

Let us now recall the well-known *fluctuation-compressibility theorem* that links the isothermal compressibility  $\kappa_T$  of equilibrium single-component many-particle ensembles at number density  $\rho$  and temperature  $T$  to infinite-wavelength density fluctuations [3]. In particular, for “open” systems in equilibrium, one has

$$\rho k_B T \kappa_T = \frac{\langle N^2 \rangle_* - \langle N \rangle_*^2}{\langle N \rangle_*} = S(\mathbf{k} = \mathbf{0}) = 1 + \rho \int_{\mathbb{R}^d} h(\mathbf{r}) d\mathbf{r}, \quad (7)$$

where  $k_B$  is Boltzmann’s constant and  $\langle \cdot \rangle_*$  denotes an average in the grand canonical ensemble.

The fluctuation-compressibility relation (7) enables one to draw useful conclusions about the hyperuniformity of equilibrium systems. Any ground state ( $T = 0$ ) in which the isothermal compressibility  $\kappa_T$  is bounded and positive must be hyperuniform because the structure factor  $S(\mathbf{k} = \mathbf{0})$  must be zero according to relation (7) [2]. More generally, we infer from (7) that if the product  $T\kappa_T$  tends to a nonnegative constant  $c$  in the limit  $T \rightarrow 0$ , then the ground-state of this system in this zero-temperature limit must be nonhyperuniform if  $c > 0$  or hyperuniform if  $c = 0$ . By the same token, this means that increasing the temperature by an arbitrarily small positive amount when a system is initially at a hyperuniform ground state will destroy perfect hyperuniformity, since  $S(\mathbf{k} = \mathbf{0})$  must deviate from zero by some small amount determined by the temperature dependence of the product  $\kappa_T T$  for small  $T$  [2]. This indirectly implies that phonons or vibrational modes for sufficiently small  $T$  generally destroy the hyperuniformity of ground states [23, 25]. Additionally, in order to have a hyperuniform system that is in equilibrium at any positive  $T$ , the isothermal compressibility must be zero, i.e., the system must be thermodynamically incompressible [2].

### B. Inverted Critical Point and Scaling Laws

The direct correlation function  $c(\mathbf{r})$  of a hyperuniform system behaves in an unconventional manner compared to that of typical liquids. This function is defined via the Ornstein-Zernike integral equation [45]:

$$h(\mathbf{r}) = c(\mathbf{r}) + \rho c(\mathbf{r}) \otimes h(\mathbf{r}), \quad (8)$$

where  $\otimes$  denotes a convolution integral. Fourier transforming (8) and solving for  $\tilde{c}(\mathbf{k})$ , the Fourier transform of  $c(\mathbf{r})$ , yields

$$\tilde{c}(\mathbf{k}) = \frac{\tilde{h}(\mathbf{k})}{S(\mathbf{k})} = \frac{\tilde{h}(\mathbf{k})}{1 + \rho \tilde{h}(\mathbf{k})}. \quad (9)$$

By definition, a hyperuniform system is one in which  $\tilde{h}(\mathbf{k} = \mathbf{0}) = -1/\rho$ , i.e., the volume integral of  $h(\mathbf{r})$  exists, implying that  $h(\mathbf{r})$  is sufficiently short-ranged in the sense that it decays to zero faster than  $|\mathbf{r}|^{-d}$ . Interestingly, this means that the denominator on the right side of (9) vanishes at  $\mathbf{k} = \mathbf{0}$  and therefore  $\tilde{c}(\mathbf{k} = \mathbf{0})$  diverges to  $-\infty$ . This behavior implies that the the volume integral of  $c(\mathbf{r})$  does not exist and hence the real-space direct correlation function  $c(\mathbf{r})$  is long-ranged, i.e., decays slower than  $|\mathbf{r}|^{-d}$ . We see that this behavior stands in diametric contrast to standard thermal critical-point systems in which the total correlation function is long-ranged and the direct correlation function is short-ranged such that its volume integral exists [38–41]. For this reason, it has been said that hyperuniform systems are at an “inverted” critical point [1]. As noted earlier, systems at thermal critical points are anti-hyperuniform.

There is a class of disordered hyperuniform systems with concomitant critical exponents [1, 2]. For such hyperuniform critical systems, the direct correlation function has the following asymptotic behavior for large  $r \equiv |\mathbf{r}|$  and sufficiently large  $d$ :

$$c(\mathbf{r}) \sim -\frac{1}{r^{d-2+\eta}} \quad (r \rightarrow \infty), \quad (10)$$

where  $(2-d) < \eta \leq 2$  is a “critical” exponent associated with  $c(\mathbf{r})$  for hyperuniform systems that depends on the space dimension. The Fourier transform of (10) yields

$$\tilde{c}(\mathbf{k}) \sim -\frac{1}{k^{2-\eta}} \quad (k \rightarrow 0), \quad (11)$$

which, when combined with (9), yields the asymptotic form of the structure factor

$$S(\mathbf{k}) \sim k^{2-\eta} \quad (k \rightarrow 0), \quad (12)$$

where  $\eta = 2 - \alpha$  and  $\alpha$  is the exponent defined in relation (3).

In what follows, it is assumed for concreteness, that the number density is the control parameter. We define the following dimensionless density:

$$\phi = \rho v_1(D/2), \quad (13)$$

where  $v_1(R)$  is given by (2) and  $D$  is a characteristic “microscopic” length scale. The direct correlation in the vicinity of a hyperuniform critical state with dimensionless density  $\phi_c$ , i.e., for  $|\phi_c - \phi| \ll 1$ , in sufficiently high dimensions has the following large- $r$  asymptotic form [1, 2]:

$$c(\mathbf{r}) \sim \frac{\exp(-|\mathbf{r}|/\xi)}{|\mathbf{r}|^{d-2+\eta}}, \quad (14)$$

where  $\xi$  is the *correlation length*. If the system approaches a hyperuniform state from below the critical density  $\phi_c$ , the correlation length and inverse of the structure factor at  $k = 0$ ,  $S^{-1}(0)$ , which is proportional to  $\tilde{c}(0)$ , are described by the following scaling laws:

$$\xi \sim \left(1 - \frac{\phi}{\phi_c}\right)^{-\nu} \quad (\phi \rightarrow \phi_c^-), \quad (15)$$

$$S^{-1}(0) \sim \left(1 - \frac{\phi}{\phi_c}\right)^{-\gamma}, \quad (\phi \rightarrow \phi_c^-), \quad (16)$$

where  $\nu$  and  $\gamma$  are nonnegative critical exponents. Observe that the exponent  $\gamma$  is a measure of how quickly a system approaches a critical point. Combination of the three previous scaling laws leads to the following interrelation between the exponents:

$$\gamma = (2 - \eta)\nu. \quad (17)$$

The specific values of the critical exponents determine the *universality* class of the hyperuniform system. It is noteworthy that all class III hyperuniform systems are at critical points with the aforementioned scaling laws. Specific examples of such a class III critical-point systems are nonequilibrium absorbing-state models [37].

### C. Growing Length Scale

Another important length scale  $\xi_c$  that can be extracted from the direct correlation function and which grows as a hyperuniform state is approached is defined by [46]

$$\xi_c = [-\tilde{c}(k=0)]^{1/d}. \quad (18)$$

Thus, we see that  $\xi_c$  is the  $d$ th root of the volume integral of the direct correlation function  $c(\mathbf{r})$ . At a hyperuniform critical point,  $\xi_c$  diverges to  $+\infty$ . It was shown that a precursor to the hyperuniform maximally random jammed (MRJ) state of sphere packings [47] under compression was evident for densities far below the jamming density was reached, as reflected by this static growing length scale [46]. The quantity  $\xi_c$  was also used to identify length scales in supercooled atomic liquid models that substantially grow as the temperature decreased [48].

### D. Hyperuniformity Index

The *hyperuniformity index*  $H$  provides a measure of the nearness of a system to a hyperuniform state, which is defined as

$$H \equiv \frac{S(0)}{S(k_p)}, \quad (19)$$

where  $k_p$  is the wavenumber  $k$  associated with the largest peak height of the angularly averaged structure factor. One may empirically deem a system to be nearly or effectively hyperuniform if  $H$  is roughly less than about  $10^{-4}$  [32]. The  $H$  index has been profitably used to quantify the effective hyperuniformity of polymer systems [49, 50], amorphous ices [51], states along the metastable extension of the hard-sphere systems away from jamming [52] and low-temperature states of “quantizer” systems [53, 54].

## III. HYPERUNIFORM AND NONHYPERUNIFORM SCALING REGIMES

For a large class of ordered and disordered systems, the number variance  $\sigma^2(R)$  has the following large- $R$  asymptotic behavior [1, 2]:

$$\sigma^2(R) = 2^d \phi \left[ A \left(\frac{R}{D}\right)^d + B \left(\frac{R}{D}\right)^{d-1} + o\left(\frac{R}{D}\right)^{d-1} \right] \quad (20)$$

where  $\phi$  is the dimensionless density given by (2) and  $o(R/D)^{d-1}$  represents terms of lower order than  $(R/D)^{d-1}$ . Moreover,  $A$  and  $B$  are “volume” and “surface-area” coefficients, respectively, which can be expressed as the following volume integrals involving the total correlation function  $h(\mathbf{r})$ , respectively:

$$\begin{aligned} A &= \lim_{|\mathbf{k}| \rightarrow 0} S(\mathbf{k}) = 1 + \rho \int_{\mathbb{R}^d} h(\mathbf{r}) d\mathbf{r} \\ &= 1 + d 2^d \phi \int_0^\infty x^{d-1} h(x) dx, \end{aligned} \quad (21)$$

$$\begin{aligned} B &= -\frac{d \Gamma(d/2) \rho}{2 \pi^{1/2} D \Gamma[(d+1)/2]} \int_{\mathbb{R}^d} |\mathbf{r}| h(\mathbf{r}) d\mathbf{r} \\ &= -\frac{d^2 2^{d-1} \Gamma(d/2) \phi}{\pi^{1/2} \Gamma[(d+1)/2]} \int_0^\infty x^d h(x) dx, \end{aligned} \quad (22)$$

and  $x = r/D$  is a dimensionless distance. Here  $h(r)$  is the radial function that depends on the distance  $r \equiv |\mathbf{r}|$ , which results from averaging the vector-dependent quantity  $h(\mathbf{r})$ , i.e.,

$$h(r) = \frac{1}{\Omega} \int_{\Omega} h(\mathbf{r}) d\Omega, \quad (23)$$

$d\Omega$  is the differential solid angle and

$$\Omega = \frac{d\pi^{d/2}}{\Gamma(1 + d/2)} \quad (24)$$

is the total solid angle contained in a  $d$ -dimensional sphere. In a perfectly hyperuniform system [1], the non-negative volume coefficient vanishes, i.e.,  $A = 0$ , implying the sum rule

$$\rho \int_{\mathbb{R}^d} h(\mathbf{r}) d\mathbf{r} = -1, \quad (25)$$



such that the surface-area coefficient  $B$  is nonnegative. Thus, such hyperuniform systems fall within class I, since the variance grows like the window surface area ( $R^{d-1}$ ). On the other hand, when  $A > 0$  and  $B = 0$ , the system is *hyposurficial*, implying the sum rule

$$\int_0^\infty x^d h(x) dx = 0. \quad (26)$$

Examples of hyposurficial systems include ideal gases, certain hard-core systems in  $\mathbb{R}^d$  [1], non-equilibrium phase transitions in amorphous ices [51], and certain systems with bounded pair interactions [55]. Appendix A provides a more general asymptotic expansion of the local number variance, which is used to derive nonhyperuniform scaling laws.

For a large class of nonhyperuniform disordered systems that are *sub-Poissonian* [56], such as fluids and colloids without particle clustering, the volume coefficient  $A$  is often larger than the magnitude of the surface-area coefficient  $B$ . For *super-Poissonian* configurations [56], such as the one described in Appendix B, the magnitude of  $B$  can be larger than  $A$ . When  $A < 1$  and  $A < B$ ,  $B$  is often positive, and the smallness of the ratio  $A/B$  measures the degree of hyperuniformity [51]. In a disordered system that is nearly hyperuniform, the inverse of this ratio,  $B/A$  enables us to ascertain hyperuniform and nonhyperuniform distance-scaling regimes of the variance  $\sigma^2(R)$  as a function of  $R$ . The crossover value of  $R_c$  between these two scaling regimes is determined by equating the first two terms of the large- $R$  asymptotic expansion of the local number variance, Eq. (20), yielding the condition

$$R_c \approx \frac{B}{A}. \quad (27)$$

For the range  $R_0 < R < R_c$ , where  $R_0 \approx \rho^{-1/d}$  (roughly, equal to the mean-nearest neighbor distance), the system exhibits hyperuniform scaling behavior, i.e., the variance is dominated by the surface-area scaling,  $R^{d-1}$ . Clearly, the crossover value  $R_c$  becomes infinite for perfectly hyperuniform systems in which case  $B/A = +\infty$ . On the other hand, for  $R > R_c$  and finite  $B/A$ , the system begins to exhibit nonhyperuniform scaling behavior, i.e., the variance is dominated by the surface-area scaling,  $R^d$ . The determination of hyperuniform scaling regimes could be especially useful in analyzing experimentally or computationally-generated systems that are necessarily of finite size  $L$  such that  $R < L/4$  [56].

#### IV. FOURIER REPRESENTATION OF SURFACE-AREA COEFFICIENT

Here we derive a Fourier representation of the surface-area coefficient  $B$  for any homogeneous many-particle system, whether hyperuniform or not, provided that the structure factor meets certain mild conditions. This representation will be especially useful when the scattering

intensity is available experimentally or if the structure factor is analytically available, as it is when solving the Ornstein-Zernike integral equation (8).

We define the Fourier transform of a function  $f(\mathbf{r})$  that depends on the vector  $\mathbf{r}$  in  $d$ -dimensional Euclidean space  $\mathbb{R}^d$  as follows:

$$\tilde{f}(\mathbf{k}) = \int_{\mathbb{R}^d} f(\mathbf{r}) \exp[-i(\mathbf{k} \cdot \mathbf{r})] d\mathbf{r}, \quad (28)$$

where  $\mathbf{k}$  is a wave vector and  $(\mathbf{k} \cdot \mathbf{r}) = \sum_{i=1}^d k_i r_i$  is the conventional Euclidean inner product of two real-valued vectors. The function  $f(\mathbf{r})$  can generally represent a tensor of arbitrary rank. When it is well-defined, the corresponding inverse Fourier transform is given by

$$f(\mathbf{r}) = \left(\frac{1}{2\pi}\right)^d \int_{\mathbb{R}^d} \tilde{f}(\mathbf{k}) \exp[i(\mathbf{k} \cdot \mathbf{r})] d\mathbf{k}. \quad (29)$$

If  $f$  is a radial function, i.e.,  $f$  depends only on the modulus  $r = |\mathbf{r}|$  of the vector  $\mathbf{r}$ , its Fourier transform is given by

$$\tilde{f}(k) = (2\pi)^{\frac{d}{2}} \int_0^\infty r^{d-1} f(r) \frac{J_{(d/2)-1}(kr)}{(kr)^{(d/2)-1}} dr, \quad (30)$$

where  $k = |\mathbf{k}|$  is the wavenumber or modulus of the wave vector  $\mathbf{k}$  and  $J_\nu(x)$  is the Bessel function of the first kind of order  $\nu$ . The inverse transform of  $\tilde{f}(k)$  is given by

$$f(r) = \frac{1}{(2\pi)^{\frac{d}{2}}} \int_0^\infty k^{d-1} \tilde{f}(k) \frac{J_{(d/2)-1}(kr)}{(kr)^{(d/2)-1}} dk. \quad (31)$$

The Fourier representation of the local number variance for statistically homogeneous media, which includes perfect crystals (under uniform translations of the crystals over their fundamental cells) [2], is given by

$$\sigma^2(R) = 2^d \phi R^d \left[ \frac{1}{(2\pi)^d} \int_{\mathbb{R}^d} S(\mathbf{k}) \tilde{\alpha}(\mathbf{k}; \mathbf{R}) d\mathbf{k} \right], \quad (32)$$

where

$$\tilde{\alpha}(k; R) = 2^d \pi^{d/2} \Gamma(1 + d/2) \frac{[J_{d/2}(kR)]^2}{k^d} \quad (33)$$

is the Fourier transform of the scaled intersection volume function  $\alpha(r; R)$ , which depends only on the magnitude of the wavevector  $k = |\mathbf{k}|$ . Using the identity

$$\frac{1}{(2\pi)^d} \int_{\mathbb{R}^d} \tilde{\alpha}(k; R) d\mathbf{k} = 1, \quad (34)$$

it follows from (32) that

$$\sigma^2(R) = 2^d \phi S_0 R^d + 2^d \phi R^d \left[ \frac{1}{(2\pi)^d} \int_{\mathbb{R}^d} [S(\mathbf{k}) - S_0] \tilde{\alpha}(k; R) d\mathbf{k} \right], \quad (35)$$

where

$$S_0 \equiv \lim_{|\mathbf{k}| \rightarrow 0} S(\mathbf{k}) = A = 1 + \rho \int_{\mathbb{R}^d} h(\mathbf{r}) d\mathbf{r}, \quad (36)$$

which implies

$$\tilde{\rho}\tilde{h}(\mathbf{k} = \mathbf{0}) = S_0 - 1. \quad (37)$$

Since  $\tilde{\alpha}(k; R)$  is a radial function, depending only on the magnitude of the wavevector, we can carry out the angular integration in the integral in (35), yielding

$$\sigma^2(R) = 2^d \phi S_0 R^d + 2^d \phi R^d \left[ \frac{d\pi^{d/2}}{(2\pi)^d \Gamma(1 + d/2)} \int_{\mathbb{R}^d} k^{d-1} [S(k) - S_0] \tilde{\alpha}(k; R) dk \right] \quad (38)$$

where the radial function  $S(k)$  is given by

$$S(k) = \frac{1}{\Omega} \int_{\Omega} S(\mathbf{k}) d\Omega. \quad (39)$$

For large  $R$ ,

$$\tilde{\alpha}(k; R) \sim 2^{d+1} \pi^{d/2-1} \Gamma(1 + d/2) \frac{\cos^2[kR - (d+1)/4]}{Rk^{d+1}}. \quad (40)$$

Combination of (38) and (40) yields the following large- $R$  asymptotic expansion:

$$\sigma^2(R) \sim 2^d \phi S_0 R^d + 2^d \phi R^{d-1} \left[ \frac{2d}{\pi} \int_0^\infty \frac{S(k) - S_0}{k^2} \cos^2\left[kR - \frac{d+1}{4}\right] dk \right] + \mathcal{O}(R^{d-3}). \quad (41)$$

Using the identity

$$\lim_{L \rightarrow \infty} \frac{1}{L} \int_0^L \cos^2\left[kR - \frac{d+1}{4}\right] dR = \frac{1}{2} \quad (42)$$

and (41), we obtain

$$\sigma^2(R) \sim 2^d \phi S_0 R^d + 2^d \phi R^{d-1} \left[ \frac{d}{\pi} \int_0^\infty \frac{S(k) - S_0}{k^2} dk \right] + \mathcal{O}(R^{d-3}). \quad (43)$$

Comparing (43) to (20) yields the desired Fourier representation of the surface-area coefficient

$$B = \frac{d}{\pi} \int_0^\infty \frac{S(k) - S_0}{k^2} dk. \quad (44)$$

Thus, this Fourier representation of the coefficient  $B$  is bounded provided that the difference  $[S(k) - S_0]$  tends to zero in the limit  $k \rightarrow 0$  faster than linear in  $k$ . Note that this condition will always be met by any structure factor that is analytic at the origin, since  $[S(k) - S_0]$  must vanish at least as fast as quadratically in  $k$  as  $k \rightarrow 0$ . Finally, we observe that if the system is hyposurficial ( $B = 0$ ), relation (44) leads to the integral condition

$$\int_0^\infty \frac{S(k) - S_0}{k^2} dk = 0, \quad (45)$$

which is the Fourier-space sum rule for hyposurficiality that corresponds to the direct-space sum rule (26).

## V. TOWARD JAMMED STATES IN EQUILIBRIUM HARD-SPHERE SYSTEMS

We recall some well-known results for the equilibrium phase behavior of identical hard spheres of diameter  $D$ . The pressure of an equilibrium hard-sphere system in any space dimension can be expressed in terms of the contact values of the direct correlation function from the right and left sides via the Ornstein–Zernike equation [57]:

$$\frac{p}{\rho k_B T} = 1 + 2^{d-1} \phi [c(D^+) - c(D^-)]. \quad (46)$$

Here the dimensionless density  $\phi$  is to be interpreted as the *packing fraction*, i.e., the fraction of space covered by the spheres. Figure 1 schematically shows the three-dimensional (3D) phase behavior in the  $\phi$ - $p$  plane. Three different isothermal densification paths by which a hard-sphere liquid may jam are shown. At sufficiently low densities, an infinitesimally slow compression of the system at constant temperature defines a thermodynamically stable liquid branch for packing fractions up to the “freezing” point ( $\phi \approx 0.494$ ). Increasing the density beyond the freezing point putatively results in an entropy-driven first-order phase transition [58, 59] to a crystal branch that begins at the melting point ( $\phi \approx 0.55$ ). Slow compression of the system along the crystal branch ends at the jammed state corresponding to the fcc lattice packing [60] with  $\phi = \pi/\sqrt{18} = 0.74048\dots$ . Rapid compressions of the liquid while suppressing some degree of local order can avoid crystal nucleation (on short time scales) and produce a range of amorphous metastable extensions of the liquid branch that jam only at their density maxima. The faster the compression rate, the lower is the jammed density. Presumably, the metastable branch produced by the most rapid compression rate with a terminal density consistent with strict jamming corresponds to the maximally random jammed (MRJ) state with  $\phi \approx 0.64$  [47, 61]. The MRJ state under the strict-jamming constraint [62, 63] is a prototypical glass [64] in that it is maximally disordered (according to a variety of order metrics) without any long-range order (Bragg peaks) and perfectly rigid, i.e., the elastic moduli are unbounded [61, 65].

In the immediate vicinity of a jammed state in  $\mathbb{R}^d$  with packing fraction  $\phi_J$ , the set of particle displacements that are accessible to the packing approaches a convex-limiting polytope (because the impenetrability constraints become linear) and free-volume theory [66–68] predicts that the pressure  $p$  has the following exact asymptotic form:

$$\frac{p}{\rho k_B T} \sim \frac{d}{1 - \phi/\phi_J} \quad (\phi \rightarrow \phi_J). \quad (47)$$

So far as the limiting polytope picture is concerned, the extremely narrow connecting filaments that in principle connect the jamming neighborhoods have so little measure that they do not overturn the free-volume leading

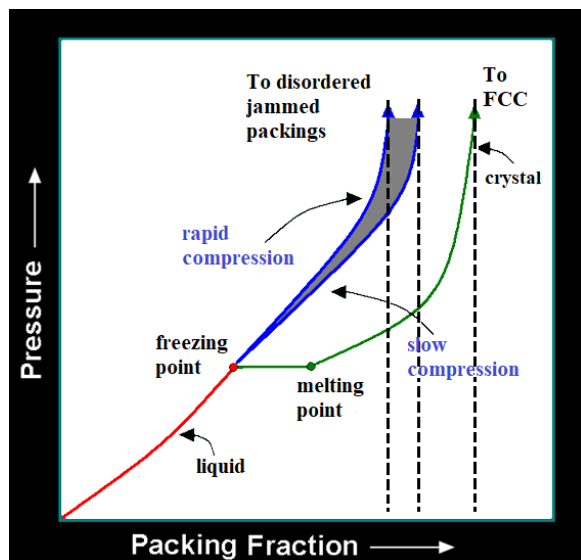


FIG. 1. The isothermal phase behavior of the 3D hard-sphere model in the pressure-packing fraction plane, as adapted from Ref. 61. An infinitesimal compression rate of the liquid traces out the thermodynamic equilibrium path (shown in red), including a discontinuity resulting from the first-order freezing transition to a crystal branch (shown in green) that ends at a maximally dense, infinite-pressure jammed state. Rapid compressions of the liquid (blue curves) generate a range of amorphous metastable extensions of the liquid branch that jam only at their density maxima, which we show here must be perfectly hyperuniform states.

behavior of the pressure, even in the infinite-system limit [61]. Although there is no rigorous proof yet for this claim, all numerical evidence strongly suggests that it is correct as the jamming state is approached either along the crystal [66, 67] or metastable branch [68]. Assuming that the system dynamics remain ergodic in the vicinity of a jammed state, we can apply the fluctuation-compressibility relation (7) along with the free-volume form (47) to yield the corresponding asymptotic relation for  $S^{-1}(0)$ :

$$S^{-1}(0) \sim \frac{d}{(1 - \phi/\phi_J)^2} \quad (\phi \rightarrow \phi_J). \quad (48)$$

Thus, we see that in the limit  $\phi \rightarrow \phi_J$ , the system becomes perfectly hyperuniform, which appears to validate a more general conjecture of Torquato and Stillinger [1], as elaborated below.

It is important to note that ergodicity condition required to obtain (48) implies that the system must be defect-free. To stress this point further, consider an fcc packing in  $\mathbb{R}^3$  at the jammed state with packing fraction  $\phi = \pi/\sqrt{18} = 0.74048\dots$ . Next, shrink each sphere by an infinitesimal uniform amount (such that the impenetrability constraints are linerizable) and randomly remove a small but statistically significant fraction of spheres so that the resulting vacancies are well-separated from one another. This vacancy-riddled packing remains in its jamming basin. Now, slowly compress it until it jams, whereby the system pressure diverges. It is known that

the structure factor  $S(\mathbf{k})$  at the origin of a nearly hyperuniform system with vacancies is proportional to the concentration of vacancies [23] and hence cannot be hyperuniform, as predicted by (48). Thus, the free-volume form for the pressure (47) cannot apply to this nonequilibrium vacancy-riddled but strictly jammed state.

More generally, Torquato and Stillinger [1] suggested that certain defect-free strictly jammed packings of identical spheres are hyperuniform. Specifically, they conjectured that any strictly jammed saturated infinite packing of identical spheres is hyperuniform. A saturated packing of hard spheres is one in which there is no space available to add another sphere. What is the rationale for such a conjecture? First, it recognizes that mechanical rigidity is a necessary but not sufficient condition for hyperuniformity. Indeed, requiring the saturation property in the conjecture eliminates the class of strictly jammed crystal states that are riddled with vacancies, as per the aforementioned example. Moreover, the conjecture excludes packings that may have a rigid backbone but possess “rattlers” (particles that are not locally jammed but are free to move about a confining cage) because a strictly jammed packing, by definition, cannot contain rattlers [61, 68]. Typical packing protocols that have generated disordered jammed packings tend to contain a small concentration of rattlers [61, 69], and hence the entire (saturated) packing cannot be deemed to be jammed. Therefore, the conjecture cannot apply to current numerically-generated disordered packings, even if the structure factor at the origin is very small, e.g., an  $H$  index of the order of  $10^{-4}$  for 3D MRJ-like sphere packing [29]. Thus, rattler-free disordered jammed sphere packings are expected to be perfectly hyperuniform. Indeed, if the free-volume theory applies along the metastable extension ending at the MRJ state, rattlers cannot be present (due to a type of constrained ergodicity on time scales much less than relaxation times) and hence should be perfectly hyperuniform. It has been suggested that the ideal MRJ state is rattler-free, implying that the packing is more disordered without the presence of rattlers [32].

The consequences of the free-volume theory requires a modification of the Torquato-Stillinger conjecture because the former eliminates defects of *any* type in the jamming limit and the saturation condition may not prohibit all defect types. For example, the saturation property may not exclude dislocations in strictly jammed crystal states. A more refined variant of the conjecture is the following statement: Any strictly jammed infinite packing of identical spheres that is defect-free is hyperuniform.

In Appendix C, we obtain exact sum rules and the exact large- $k$  asymptotic behaviors of the structure factors of certain general packings of identical spheres in  $\mathbb{R}^d$ , whether in equilibrium or not.

## VI. EQUILIBRIUM HARD RODS

We first structurally characterize one-dimensional systems of identical hard rods of length  $D$  in equilibrium as a function of the packing fraction  $\phi$  up to the jammed, hyperuniform state ( $\phi = 1$ ). This hyperuniform state is the integer lattice  $\mathbb{Z}$  and hence cannot be regarded to be a critical hyperuniform state, as described in Sec. II B.

Percus [70] obtained the following exact expression for the direct correlation function for an equilibrium hard-rod system at packing fraction  $\phi$ :

$$c(r) = -\Theta(D - r) \frac{1 - \phi r/D}{(1 - \phi)^2} \quad (49)$$

where  $\Theta(x)$  is the Heaviside step function. Combination of this relation with (46) yields the well-known expression for the pressure of the hard-rod system [71]:

$$\frac{p}{\rho k_B T} = \frac{1}{1 - \phi}, \quad (50)$$

which we see takes the free-volume form (47) for the entire range of packing fractions, not just near the jammed state  $\phi_J = 1$ , which must be hyperuniform. The Fourier transform of  $c(r)$  is given by

$$\tilde{c}(k) = \frac{2[\phi(\cos(kD) - 1) + kD \sin(kD)(\phi - 1)]}{(1 - \phi)^2 (kD)^2}. \quad (51)$$

Using (9), the corresponding structure factor is given by

$$S(k) = \frac{1}{1 - \frac{2\phi[\phi(\cos(kD) - 1) + kD \sin(kD)(\phi - 1)]}{(1 - \phi)^2 (kD)^2}}. \quad (52)$$

It is seen that the asymptotic large- $k$  behavior of  $S(k)$  is consistent with the general expression (C6) for  $d = 1$ , where the contact value  $g_2(D^+) = (1 - \phi)^{-1}$  is bounded for all  $\phi$ , except at its maximal value  $\phi = 1$ .

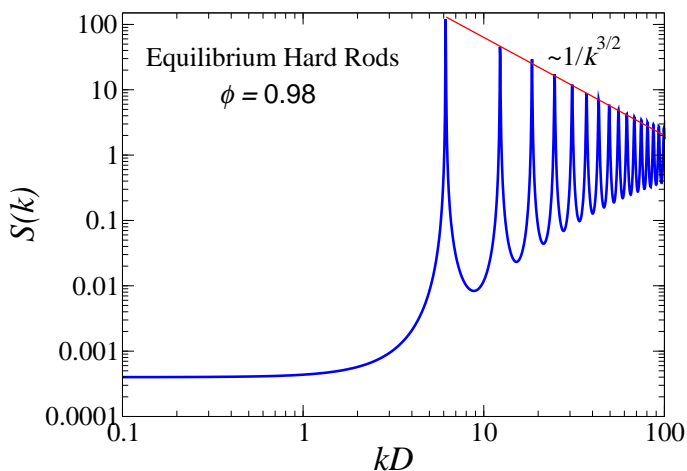


FIG. 2. The structure factor  $S(k)$  versus the dimensionless wavenumber  $kD$  for a equilibrium hard-rod system near the jammed state ( $\phi = 0.98$ ). The envelope of the largest peak values decays with wavenumber approximately as the power law  $1/k^{3/2}$ .

The structure factor  $S(k)$  is plotted in Fig. 2 for the hard-rod system near the jammed state with  $\phi = 0.98$ . At such high densities, its peak values occur at wavenumbers that are approximately integer multiples of  $2\pi/D$ , which is exactly the case for the integer lattice (jammed state) with lattice constant  $D$ . The envelope of the largest peak values decays with wavenumber approximately as the power law  $1/k^{3/2}$ . It immediately follows from (52) that the volume coefficient  $A$ , defined by (21), is exactly given by

$$A = S(0) = (1 - \phi)^2 \quad (53)$$

The surface-area coefficient  $B$  is easily obtained for all  $\phi$  from its Fourier representation (44) and use of the exact structure factor formula (52) by high-precision numerical integration. These results for  $B$  are in excellent agreement with previous results using the direct-space representation of  $B$  [1]. A simple and highly accurate formula for  $B$  is given by

$$B = \frac{\phi}{12}(6 - 8\phi + 3\phi^2). \quad (54)$$

This formula is obtained by using exact results at low and high packing fractions and assuming that  $B$  is a cubic polynomial in  $\phi$  (without a constant term). Specifically, the linear and quadratic terms are determined by the exact expansion of  $S(k) - S_0$  in powers of  $\phi$  through second order in  $\phi$ , as determined from the exact formula (52). The remaining cubic term is found by using the fact that  $B$  is exactly equal to  $1/12$  for the integer lattice at  $\phi = 1$  [1]. Thus, combination of the aforementioned formulas for  $A$  and  $B$ , yields the following excellent approximation for the ratio

$$\frac{B}{A} = \frac{\phi(6 - 8\phi + 3\phi^2)}{12(1 - \phi)^2}. \quad (55)$$

The ratio  $B/A$  is plotted in Fig. 3 as a function of  $\phi$ . It is seen that  $B$  is about ten times larger than  $A$  at  $\phi = 0.9$  and the ratio dramatically diverges to infinity as  $\phi$  tends to unity. For example, at  $\phi = 0.99$ ,  $B$  is about 842 times larger than  $A$ . Referring to Sec. A, the magnitude of the ratio  $B/A$  determines the hyperuniformity scaling regime for the local number variance  $\sigma^2(R)$  to be those window radii in the range  $\mathcal{O}(\rho^{-1/d}) < R < R_c = B/A$ . For  $R$  beyond  $\mathcal{O}(B/A)$ , the variance should display nonhyperuniform scaling of the number variance. These scaling regimes are verified in the plot of the variance at  $\phi = 0.99$  shown in Fig. 4. The actual variance, as determined from the exact relations (32) and (52), at such a high packing fraction is characterized by small-scale fluctuations around some average values, and because such variations visually obscure the scaling regimes, we considered employing the cumulative running average, defined in Ref. [72], to smooth out the small-scale oscillations around the global values. Because the cumulative average plot on the scales shown in Fig. 4 is very similar to one obtained from the asymptotic expansion (20), we employ the later, for simplicity, to show the scaling regimes.



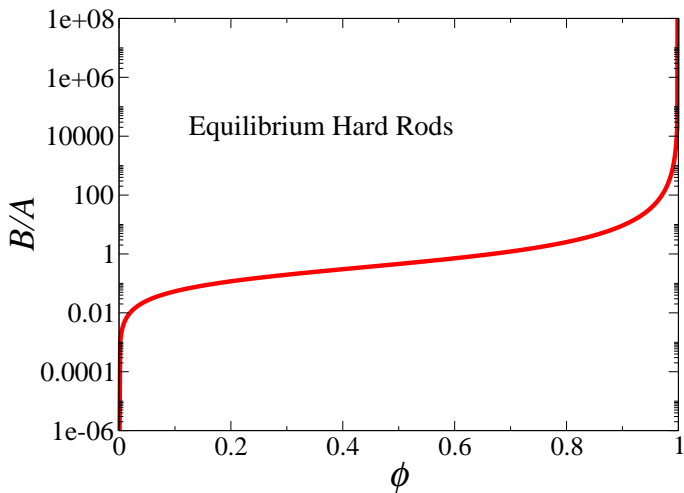


FIG. 3. The ratio of the surface-area coefficient to volume coefficient,  $B/A$ , as a function of the packing fraction  $\phi$  for equilibrium hard-rod systems.

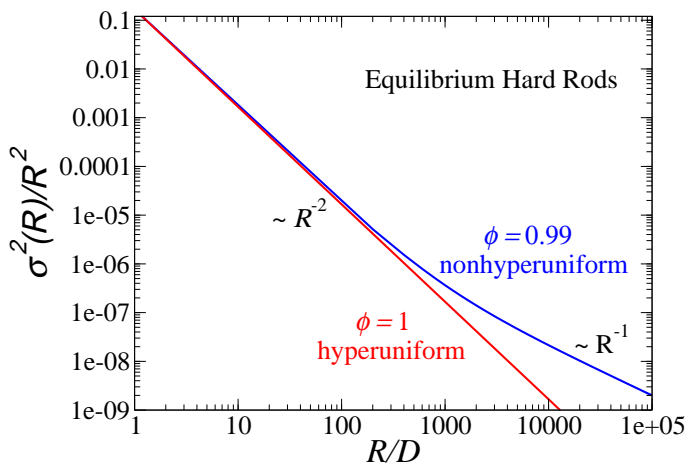


FIG. 4. The scaled variance  $\sigma^2(R)/R^2$  versus  $R/D$ , as computed from relation (20), for the jammed hyperuniform state with  $\phi = 1$  (as found in Ref. [1]) and for a nonhyperuniform state near jamming with  $\phi = 0.99$ , where  $R_c = B/A = 841.7474996$ . Because the variance is bounded for the hyperuniform state [1],  $\sigma^2(R)/R^2$  decreases with  $R$  for large  $R$  like  $1/R^2$ .

It easily follows from formula (52) that the largest peak value of the structure factor  $S(k_p)$  through first-order in the packing fraction is exactly given by

$$\begin{aligned} S(k_p) &= 1 - \frac{\sin(k_p D)}{k_p D} \phi + \mathcal{O}(\phi^2) \\ &= 1 + (0.434464192 \dots) \phi + \mathcal{O}(\phi^2), \end{aligned} \quad (56)$$

where

$$k_p D = \frac{3}{4}\pi + \frac{1}{4}\sqrt{9\pi^2 - 16} = 4.489654702 \dots \quad (57)$$

It is highly nontrivial to derive an analytical expression for  $S(k_p)$  for arbitrary  $\phi$ . Of course, we know that  $S(k_p)$

must increase as  $\phi$  increases and diverges in the limit that the jamming density is approached from below, i.e.,  $\phi \rightarrow 1^-$ , which should be distinguished from the case when  $\phi = 1$  in which  $S(k)$  consists of Dirac delta functions located at wavenumbers that are multiples of  $2\pi/D$ . The first peak value of the structure factor, which is also the largest value, at a fixed value of the packing fraction is plotted in Fig. 5 as a function of  $\phi$ , which of course must diverge at the hyperuniform jammed state  $\phi = 1$ . The following rational function provides an excellent fit to the data for all  $\phi$  up to the jamming density:

$$S(k_p) = \frac{1 + a_1\phi + a_2\phi^2 + a_3\phi^3}{(1 - \phi)^2}, \quad (58)$$

where  $a_1 = -1.565536$ ,  $a_2 = 0.470399$  and  $a_3 = 0.196196$ . This fit uses the exact small- $\phi$  expansion (56) to ascertain the coefficient  $a_1$ . This accurate approximation when combined with exact formula (53) for  $S(0)$  yields the following expression for the hyperuniformity index:

$$H = \frac{(1 - \phi)^4}{1 + a_1\phi + a_2\phi^2 + a_3\phi^3}, \quad (59)$$

which is plotted in Fig. 6 as function of  $\phi$ .

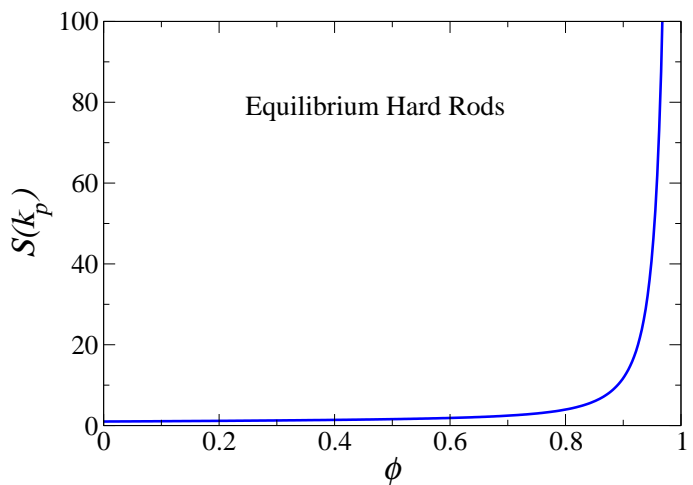


FIG. 5. The largest peak value of the structure factor  $S(k_p)$  versus the packing fraction  $\phi$  for equilibrium hard-rod systems.

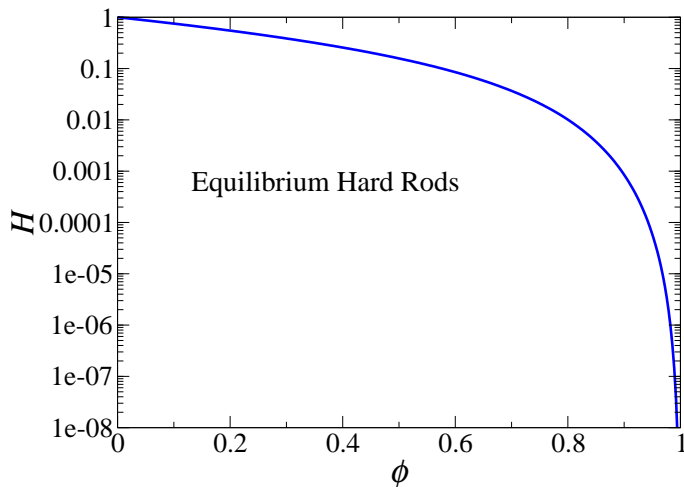


FIG. 6. The hyperuniform index  $H$  versus the packing fraction  $\phi$  for equilibrium hard-rod systems. The rapid growth of  $\xi_c$  with increasing packing fraction is readily apparent.

Using (51), it immediately follows that the length scale  $\xi_c$ , defined by (18), for equilibrium hard rods is given by

$$\xi_c = -\tilde{c}(k=0) = \frac{(2-\phi)D}{(1-\phi)^2}. \quad (60)$$

Figure 7 clearly shows that this length scale grows appreciably with increasing packing fraction. It is already about an order of magnitude greater than the length of a rod  $D$  at  $\phi = 0.6$  and rapidly takes on even larger values as  $\phi$  increases further, eventually diverging to infinity in the limit  $\phi \rightarrow 1$ .

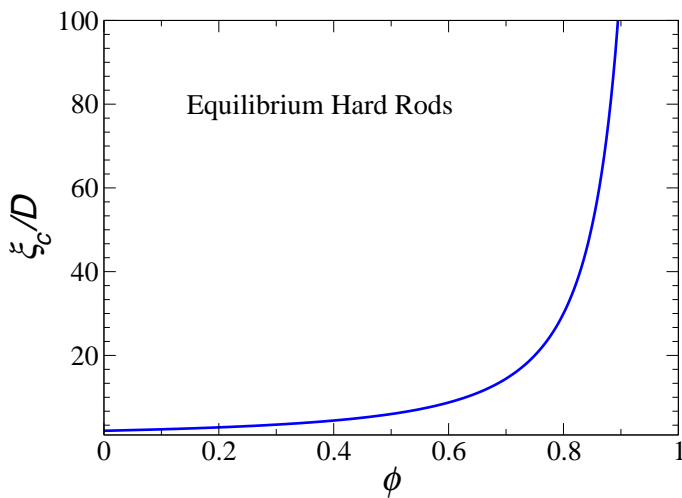


FIG. 7. The dimensionless length scale  $\xi/D$  versus the packing fraction  $\phi$  for equilibrium hard-rod systems.

It is useful to compare and contrast the growth rate of the three descriptors  $B/A$ ,  $\xi_c$  and  $H^{-1}$  as the packing fraction  $\phi$  increases and approaches the jammed hyperuniform state. We see that the numerators of the formulas (55) and (60) for moderate to high values of  $\phi$  are of

order unity, and hence  $B/A$  and  $\xi_c$  have the same scaling behavior as the hyperuniform state of the hard-rod system is approached, namely,

$$\frac{B}{A} \sim \frac{\xi_c}{D} \sim \frac{1}{(1-\phi)^2}. \quad (61)$$

This is to be contrasted with the inverse of the hyperuniformity index  $H^{-1}$ , which grows exponentially faster, i.e., we see from (6) that it grows like the square of the other two quantities:

$$H^{-1} \sim \left(\frac{B}{A}\right)^2 \sim \left(\frac{\xi_c}{D}\right)^2 \sim \frac{1}{(1-\phi)^4}. \quad (62)$$

## VII. STICKY HARD SPHERES

We utilize a particular  $g_2$ -invariant process to analytically study the approach of another disordered system to a hyperuniform but unjammed state as a function of the relevant control parameter, the number density. A  $g_2$ -invariant process is one in which a chosen nonnegative form for the pair correlation function  $g_2$  remains invariant over a nonvanishing density range while keeping all other relevant macroscopic variables fixed [1, 73]. The upper limiting “terminal” density is the point above which the nonnegativity condition on the structure factor, i.e.,  $S(\mathbf{k}) \geq 0$  for all  $\mathbf{k}$ , would be violated. Thus, at the terminal or critical density, the system is hyperuniform if the minimum in  $S(\mathbf{k})$  occurs at the origin and it is realizable. This optimization problem has deep connections to the sphere-packing problem. Specifically, it is the linear program (LP) lower bound on the maximal packing density that is dual to the Elkies-Cohn LP upper bound formulation [74]. A certain  $g_2$ -invariant test function was employed to conjecture that the densest sphere packings in very high space dimensions are disordered, rather than ordered as in low dimensions [75].

Here we specifically consider the  $g_2$ -invariant process defined by a pair correlation function that imposes a hard-core constraint via a unit step function plus a delta function contribution that acts at contact  $r = D$ :

$$g_2(r) = \Theta(r - D) + \frac{Z}{\rho s_1(D)} \delta(r - D), \quad (63)$$

where  $Z$  is the nonnegative average contact coordination number and

$$s_1(r) = \frac{d\pi^{d/2} r^{d-1}}{\Gamma(1 + d/2)} \quad (64)$$

is the surface area of a sphere of radius  $r$ . It was previously shown that this “sticky-sphere” pair correlation function is numerically realizable, to an excellent approximation, up to the hyperuniform terminal packing fraction for  $d = 2$  (see Fig. 8), implying that such pair correlation functions are also realizable in all higher dimensions, as dictated by the *decorrelation principle* [75].

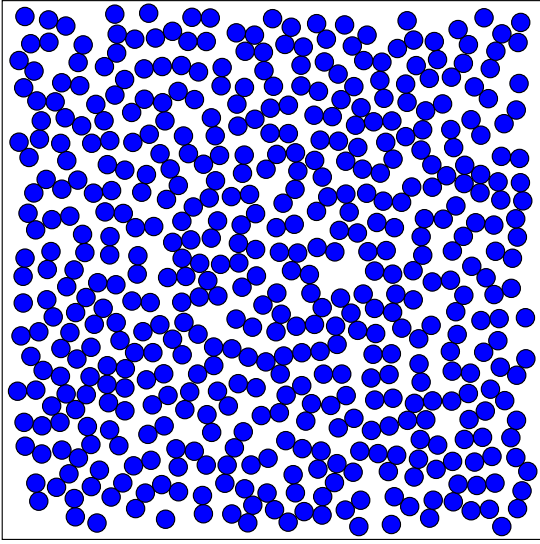


FIG. 8. A numerically generated two-dimensional configuration of 500 “sticky” hard disks that realizes the step plus delta function pair correlation function at the terminal packing fraction  $\phi_c = 1/2$ , as adapted from Ref. [76]. This critical hyperuniform state consists only of dimers, i.e.,  $Z = 1$ , and hence is unjammed, in contrast to hyperuniform states in the phase diagram of hard spheres, as shown in Fig. 1.

Here we collect previously established key results for this  $g_2$ -invariant process [1, 73] in order to characterize how such systems for any  $d$  approach a hyperuniform state as the packing fraction increases up to the critical terminal value  $\phi_c$ . It was shown that

$$Z = \frac{2^d d}{d+2} \phi \quad (65)$$

is obeyed in order to constrain the location of the minimum of the structure factor to be at  $\mathbf{k} = \mathbf{0}$ , where the packing  $\phi$  lies in the range  $0 \leq \phi \leq \phi_c$ , and

$$\phi_c = \frac{d+2}{2^{d+1}} \quad (66)$$

is the terminal or critical packing fraction, which has the same asymptotic form as a lower bound on the maximal packing density for lattice packings derived by Ball [77]. At the hyperuniform critical point, the contact number  $Z_c = d/2$ , indicating that such sticky-sphere systems are never jammed in any dimension.

The corresponding structure factor for any  $d$  and  $\phi$  in the range  $0 \leq \phi \leq \phi_c$  is given by

$$S(k) = 1 + \frac{2^{d/2} \Gamma(2 + d/2)}{(kD)^{(d/2)-1}} \left( \frac{\phi}{\phi_c} \right) \left[ \frac{J_{(d/2)-1}(kD)}{d+2} - \frac{J_{d/2}(kD)}{kD} \right]. \quad (67)$$

An important mathematical property of the structure factor for such sticky hard spheres is that its extrema for a fixed  $d$  are independent of the packing fraction. For example, for  $d = 2$  and  $d = 5$ ,  $k_p D = 6.38015\dots$  and  $k_p D = 8.18255\dots$ , respectively. It is seen that the

asymptotic large- $k$  behavior of  $S(k)$  is consistent with the general expression (C10) for any  $d$ , where  $Z$  is given by (65). Relation (67) leads to the power law

$$S^{-1}(0) = \left( 1 - \frac{\phi}{\phi_c} \right)^{-1}, \quad \phi \rightarrow \phi_c^-, \quad (68)$$

which upon comparison to (16) yields the critical exponent  $\gamma = 1$ . Figure 9 shows the structure factor  $S(k)$  versus  $kD$  for sticky hard spheres for  $d = 2$  and  $d = 5$  at their respective hyperuniform states. We see that structure factor reflects strong decorrelation in going from two to five dimensions, which is consistent with the decorrelation principle [75].

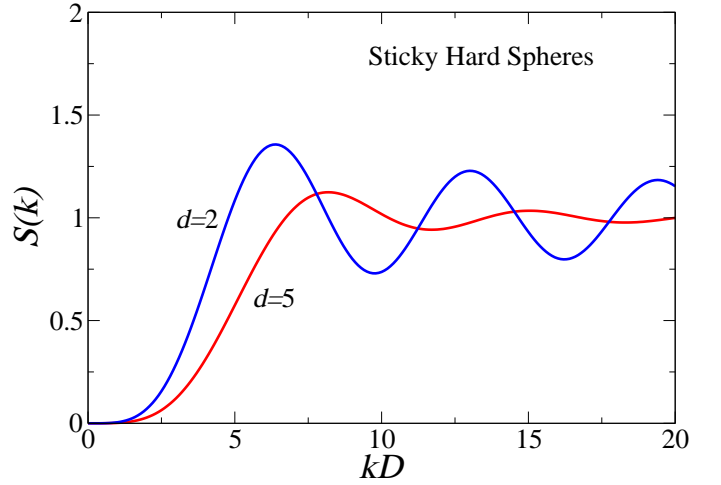


FIG. 9. The structure factor  $S(k)$  versus the dimensionless wavenumber  $kD$  for sticky hard spheres in two and five dimensions at their respective hyperuniform states, i.e.,  $\phi = \phi_c$ , where  $\phi_c$  is given by (66).

In any space dimension  $d$ , the volume and surface-area coefficients for  $0 \leq \phi \leq \phi_c$  are respectively given by

$$A = S(k=0) = 1 - \frac{\phi}{\phi_c} \quad (69)$$

and

$$B = \frac{d^2 \Gamma(d/2)}{8 \sqrt{\pi} \Gamma((d+3)/2)} \frac{\phi}{\phi_c}. \quad (70)$$

Thus, ratio  $B/A$  is given by

$$\frac{B}{A} = \frac{d^2 \Gamma(d/2)}{8 \sqrt{\pi} \Gamma((d+3)/2)} \frac{\phi/\phi_c}{(1 - \phi/\phi_c)}. \quad (71)$$

We see that apart from  $d$ -dimensional constants, the behavior of the ratio  $B/A$  is exactly the same across dimensions when the packing fraction  $\phi$  is scaled by the terminal packing fraction  $\phi_c$ . The ratio  $B/A$  versus  $\phi$  is plotted in Fig. 10 for  $d = 2$  and  $d = 5$  for all  $\phi$  up to their respective critical points.

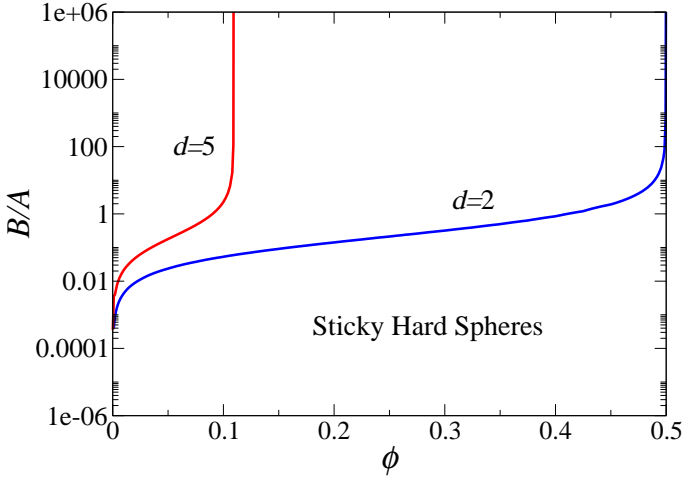


FIG. 10. The ratio of the surface-area coefficient to volume coefficient,  $B/A$ , as a function of the packing fraction  $\phi$  for sticky hard spheres in two and five dimensions.

We see from Fig. 9 that the peak value of the structure factor is not strongly dependent on the space dimension and is of order unity. Thus, the hyperuniformity index  $H$  is primarily determined by the inverse of  $A$  [cf. 69)] and so

$$H \sim \frac{1}{1 - \phi/\phi_c}. \quad (72)$$

The actual values of  $H$  are plotted in Fig. 11 as a function of  $\phi$  for  $d = 2$  and  $d = 5$  up to their respective critical points.

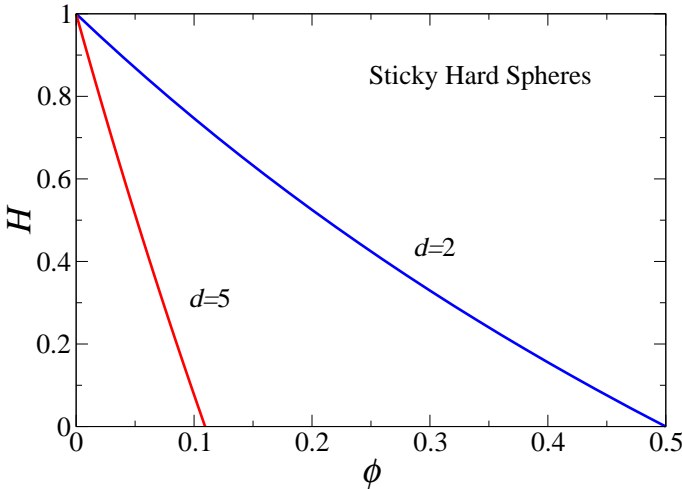


FIG. 11. The hyperuniformity index  $H$  as a function of the packing fraction  $\phi$  for sticky hard spheres in two and five dimensions.

Combination of (9) and (67) yields the following expression for the the Fourier transform of the direct cor-

relation for sticky spheres:

$$\tilde{c}(k) = \frac{\frac{(2\pi)^{d/2} D^d}{(kD)^{(d/2)-1}} \left[ \frac{J_{(d/2)-1}(kD)}{d+2} - \frac{J_{d/2}(kD)}{kD} \right]}{1 + \frac{2^{d/2} \Gamma(2 + d/2)}{(kD)^{(d/2)-1}} \left( \frac{\phi}{\phi_c} \right) \left[ \frac{J_{(d/2)-1}(kD)}{d+2} - \frac{J_{d/2}(kD)}{kD} \right]} \quad (73)$$

It immediately follows that at zero wavenumber, we have

$$\tilde{c}(0) = -2v_1(D) \left( 1 - \frac{\phi}{\phi_c} \right)^{-1}, \quad (74)$$

and, hence, the length scale defined by (18) yields

$$\xi_c = [2v_1(D)]^{1/d} \left( 1 - \frac{\phi}{\phi_c} \right)^{-1/d}, \quad (75)$$

indicating that it grows more slowly as the space dimension increases. Figure 7 shows how the length scale  $\xi_c$  grows with  $\phi$  for  $d = 2$  and  $d = 3$ .

The length scale  $\xi_c$  should be contrasted with the correlation length  $\xi$ , defined by (15), which, when combined with relation (74), yields

$$\xi = \frac{D}{[8(d+2)(d+4)\phi_c]^{1/4}} \left( 1 - \frac{\phi}{\phi_c} \right)^{-1/4}, \quad \phi \rightarrow \phi_c \quad (76)$$

Comparison of (76) to the power law (15) yields the exponent  $\nu = 1/4$ . It should not go unnoticed that since the exponents  $\gamma$ ,  $\eta$  and  $\nu$  are either integers or a simple fraction, independent of dimension, these systems always behave in a mean-field manner at their critical points.

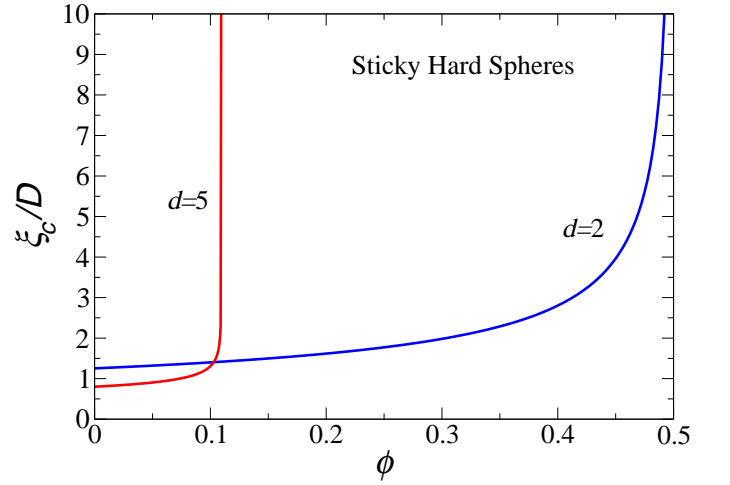


FIG. 12. The dimensionless length scale  $\xi_c/D$  versus the packing fraction  $\phi$  for sticky hard spheres in two and five dimensions.

All three descriptors  $B/A$ ,  $H^{-1}$  and  $\xi_c$  are increasing functions of the packing fraction  $\phi$ , but how do they correlate with one another? From formulas (71) and (72), we see  $B/A$  and  $H^{-1}$  have the same scaling behavior as



the critical hyperuniform state of the sticky hard-system is approached, namely,

$$\frac{B}{A} \sim H^{-1} \sim \frac{1}{(1 - \phi/\phi_c)}. \quad (77)$$

According to (75), the length scale  $\xi_c$  for  $d \geq 2$  grows more slowly than the other two quantities as the critical state is approached, i.e.,

$$(\xi_c)^d \sim \frac{B}{A} \sim H^{-1}. \quad (78)$$

### VIII. STEALTHY DISORDERED GROUND STATES

We are also interested in theoretically understanding how vibrational modes in excited low-temperatures states of matter impact the approach to ground states, which are necessarily hyperuniform (see Sec. II A), as the temperature  $T$  tends to zero. For this purpose, we consider stealthy hyperuniform many-particle systems [24, 78], which are a subclass of class I hyperuniform systems [25] in which the structure factor is zero for a range of wavevectors around the origin, i.e.,

$$S(\mathbf{k}) = 0 \quad 0 \leq |\mathbf{k}| \leq K, \quad (79)$$

where  $K$  is some positive constant. Such systems are called “stealthy” because they completely suppress single scattering of incident radiation for the wave vectors within an exclusion sphere of radius  $K$  centered at the origin in Fourier space. It has been shown that certain bounded (soft) long-ranged pair interactions have classical ground states that are stealthy and hyperuniform [25]. The nature of the ground-state configuration manifold (e.g., the degree of order) associated with such stealthy pair potentials depends on the number of constrained wave vectors. The dimensionless parameter  $\chi$  measures the relative fraction of constrained degrees of freedom compared to the total number of degrees of freedom and, counterintuitively, is inversely proportional to the number density [25]; specifically, it is explicitly given by the formula

$$\rho \chi = \frac{v_1(K)}{2d(2\pi)^d}, \quad (80)$$

where  $v_1(K)$  the volume of a  $d$ -dimensional sphere of radius  $K$  [cf. Eq. (2)]. For  $d = 2$  and  $d = 3$ , the ground states are disordered for  $0 \leq \chi < 1/2$ . At  $\chi = 1/2$ , there is a phase transition to a crystal phase. The “collective-coordinate” optimization procedure represents a powerful approach to generate numerically disordered stealthy hyperuniform many-particle systems [24, 25, 78].

A statistical-mechanical theory for disordered stealthy ground states has been formulated in the canonical ensemble in the zero-temperature limit. By exploiting an ansatz that the entropically favored (most probable)

stealthy ground states in the canonical ensemble behave like “pseudo” equilibrium hard-sphere systems in Fourier space with an “effective packing fraction”  $\phi$  that is proportional to  $\chi$ , one can employ well-established integral-equation formulations for the pair correlation function of hard spheres in direct space [3, 57] to obtain accurate theoretical predictions for  $g_2(\mathbf{r}; \phi)$  and  $S(\mathbf{k}; \chi)$  for a moderate range of  $\chi$  about  $\chi = 0$  [25], i.e.,

$$S(\mathbf{k}; \chi) = g_2^{HS}(\mathbf{r} = \mathbf{k}; \phi). \quad (81)$$

For example, the total correlation function  $h(r)$  in the limit  $\chi \rightarrow 0$  for any  $d$ , which is exactly given by

$$\rho h(r) = - \left( \frac{K}{2\pi r} \right)^{d/2} J_{d/2}(Kr) \quad (\chi \rightarrow 0), \quad (82)$$

corresponds to the following unit-step function for the structure factor:

$$S(\mathbf{k}) = \Theta(k - K) \quad (\chi \rightarrow 0). \quad (83)$$

Our interest in this paper are the excited states associated with the long-ranged stealthy potentials [25] close to the ground states, i.e., when the absolute temperature  $T$  is small. It was shown that the structure factor at the origin  $S(0)$  varies linearly with  $T$  for excited states. Importantly, this positive value of  $S(0)$  is the uniform value of  $S(\mathbf{k})$  for  $0 \leq |\mathbf{k}| \leq K$  for the special case of the step-function power-law potential for small  $\chi$ , which was verified by simulation results in various dimensions [25]. Because we are interested in qualitative trends as the disordered ground state is approached as the temperature is decreased, it suffices for our purposes to consider the following simple form for the structure factor at positive but small temperatures and sufficiently small  $\chi$ :

$$S(\mathbf{k}) = T^* \Theta(K - k) + \Theta(k - K), \quad (84)$$

where  $T^*$  is a dimensionless temperature that is much smaller than unity. The form (84) is obtained by combining the aforementioned uniform value for  $0 \leq |\mathbf{k}| \leq K$  with the ground state structure factor as  $\chi$  tends to zero, i.e., Eq. (83).

It follows from (21) and (84) that the volume coefficient is given by

$$A = T^* \quad (85)$$

Moreover, substitution of (84) into the Fourier representation of the surface-area coefficient (44) yields

$$B = \frac{d}{\pi K} (1 - T^*) \quad (86)$$

Thus, ratio  $B/A$  is given by

$$\frac{B}{A} = \frac{d}{\pi K} \frac{(1 - T^*)}{T^*}, \quad (87)$$

which is plotted in Fig. 13 as a function of the inverse of  $T^*$  for selected space dimensions. We see that at fixed

temperature, the ratio  $B/A$  increases with the space dimension. From relation (84), we see that the peak value of the structure factor is trivially unity ( $S(k_p) = 1$ ), and hence the hyperuniformity index is simply linear in  $T^*$ , i.e.,

$$H = T^*. \quad (88)$$

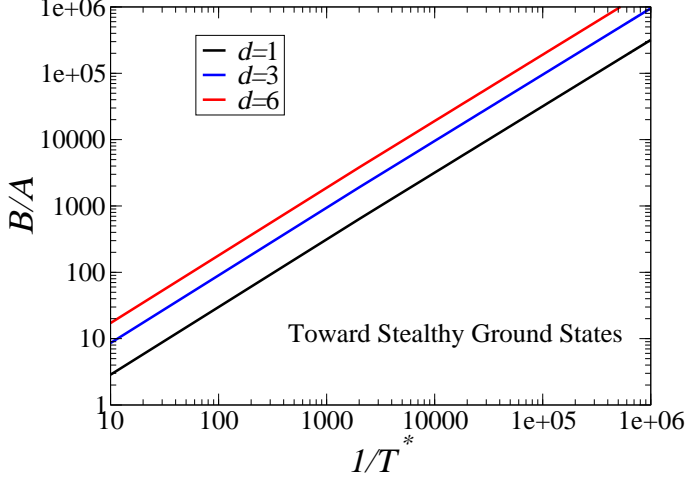


FIG. 13. The ratio of the surface-area coefficient to volume coefficient,  $B/A$ , as a function of the inverse of the dimensionless temperature  $1/T^*$  for excited states associated with the long-ranged stealthy pair potential for dimensions  $d = 1, 3$  and  $6$ .

Combination of (9) and (84) yields the following expression for the the Fourier transform of the direct correlation function for the excited states:

$$\rho\tilde{c}(\mathbf{k}) = (1 - T^*)\Theta(K - k). \quad (89)$$

Thus, evaluating this relation at zero wavenumber and use of (9) yields the length scale

$$\xi_c = (2\pi) \left[ \frac{2d\chi}{v_1(K)} \right]^{1/d} \left( \frac{1}{T^*} - 1 \right)^{1/d}. \quad (90)$$

This length scale is plotted in Fig. 14 as a function of the inverse temperature for selected space dimensions.

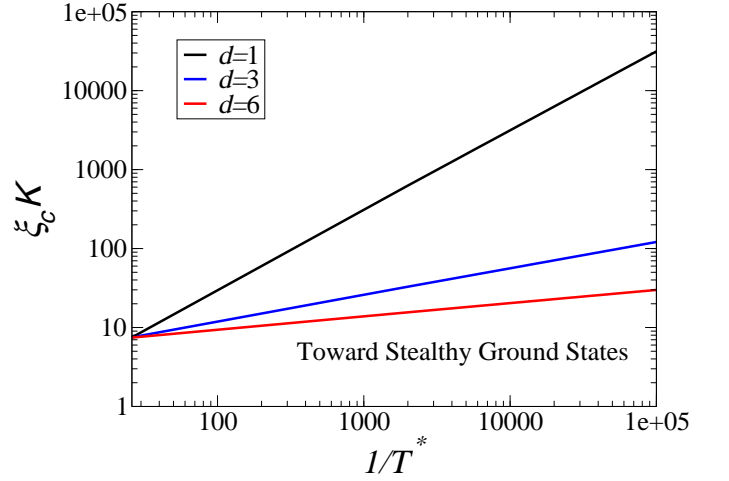


FIG. 14. The dimensionless length scale  $\xi_c K$  versus the inverse of the dimensionless temperature  $1/T^*$  for excited states associated with the long-ranged stealthy pair potential for dimensions  $d = 1, 3$  and  $6$ .

The three descriptors  $B/A$ ,  $H^{-1}$  and  $\xi_c$  are increasing functions of the inverse temperature. From formulas (87) and (72), we observe that  $B/A$  and  $H^{-1}$  have the same scaling behavior as the inverse temperature tends to infinity, i.e., the disordered hyperuniform ground state is approached, namely,

$$\frac{B}{A} \sim H^{-1} \sim \frac{1}{T^*}. \quad (91)$$

This is to be contrasted with the generally slower growth rate of  $\xi_c$  with  $T^*$  for  $d \geq 2$ , i.e.,

$$(\xi_c)^d \sim \frac{B}{A} \sim H^{-1}, \quad (92)$$

where we have used relation (90).

## IX. CONCLUSIONS AND DISCUSSION

We have derived a Fourier representation of the surface-area coefficient  $B$  in terms of the structure factor  $S(\mathbf{k})$ , which is especially useful when scattering information is available experimentally or theoretically. In a disordered system that is nearly hyperuniform, we showed that the ratio of surface-area to volume coefficients,  $B/A$ , enables one to ascertain hyperuniform and nonhyperuniform distance-scaling regimes of the variance  $\sigma^2(R)$  as a function of  $R$  as well as the corresponding crossover distance between these regimes. While the analysis of the ratio  $B/A$  was applied to systems that ultimately approached a class I hyperuniform state, the corresponding extensions to other hyperuniformity classes is very straightforward.

Using the ratio  $B/A$ , as well as other diagnostic measures of hyperuniformity, including the hyperuniformity index  $H$  and the direct-correlation function length scale

$\xi_c$ , we characterized the structure of three different exactly solvable models as a function of the relevant control parameter, either density or temperature, with end states that are perfectly hyperuniform. In the case of the sticky hard-sphere and stealthy models, we studied the effect of dimensionality. For all three models, we showed that these diagnostic hyperuniformity measures are positively correlated with one another. Thus, the quantities  $H$  and  $\xi_c$  can also be employed to infer the hyperuniform and nonhyperuniform distance-scaling regimes. This capacity to determine hyperuniform scaling regimes is expected to be of great utility in analyzing experimentally- or computationally-generated samples that are necessarily of finite size.

In the same way that there is no perfect crystal, due to the inevitable presence of imperfections, such as vacancies and dislocations, there is no “perfect” hyperuniform system in laboratory practice, whether it is ordered or not [23]. It is clear that the same diagnostic measures explored in the present work can be used to detect the degree to which such “imperfect” nearly hyperuniform systems deviate from perfect hyperuniformity.

We showed that the free-volume theory of the pressure of equilibrium packings of identical hard spheres that approach a strictly jammed state, either along the stable crystal or metastable disordered branch, dictates that such end states be exactly hyperuniform. This implies that the packing on approach to the jammed state must be ergodic in a generalized sense and hence free of any defects, e.g., vacancies or dislocations along the crystal branch or rattlers along the metastable fluid branch. It is an outstanding problem for future research to place these implications of free-volume theory for the hyperuniformity of strictly jammed packings on a firmer rigorous theoretical foundation.

### Appendix A: Number Variance Scalings for Nonhyperuniform Systems

The local number variance  $\sigma_N^2(R)$  is generally a function that can be decomposed into a global part that grows with the window radius  $R$  and a local part that oscillates on small length scales (e.g., mean nearest-neighbor distance) about the global contribution. The more general large- $R$  asymptotic formula for the variance is given by [2]

$$\sigma^2(R) = 2^d \phi \left[ A_N(R) \left(\frac{R}{D}\right)^d + B_N(R) \left(\frac{R}{D}\right)^{d-1} + o\left(\frac{R}{D}\right)^{d-1} \right] \quad (\text{A1})$$

where the  $R$ -dependent volume and surface-area coefficients are respectively given by

$$A_N(R) = 1 + \frac{\phi}{v_1(D/2)} \int_{|\mathbf{r}| \leq 2R} h(\mathbf{r}) d\mathbf{r} \quad (\text{A2})$$

and

$$B_N(R) = -\frac{\phi d \Gamma(d/2)}{2 \pi^{1/2}, D v_1(D/2) \Gamma[(d+1)/2]} \int_{|\mathbf{r}| \leq 2R} h(\mathbf{r}) |\mathbf{r}| d\mathbf{r}. \quad (\text{A3})$$

Observe that when the volume coefficient  $A_N(R)$  and surface-area coefficient  $B_N(R)$  converge in the limit  $R \rightarrow \infty$ , they are equal to the constants  $A$  and  $B$ , defined by (21) and (22), respectively. For this reason,  $A$  and  $B$  are called the *global* volume and surface-area coefficients, respectively [2].

An anti-hyperuniform system is one in which the exponent  $\alpha$  [cf. (3)] is negative  $\alpha < 0$ , resulting in a structure factor that diverges in the zero-wavenumber limit. The corresponding total correlation function  $h(\mathbf{r})$  decays like  $1/r^{d+\alpha}$  for large  $r \equiv |\mathbf{r}|$ . This power-law tail controls the growth rate of  $A_N(R)$  with  $R$ ; specifically, carrying out the integration in (A2) yields

$$A_N(R) \sim R^{-\alpha}. \quad (\text{A4})$$

Substitution of this scaling behavior in the leading-order term of (A1) gives that the local number variance for an anti-hyperuniform system scales like  $\sigma^2(R) \sim R^{d-\alpha}$ , which proves the anti-hyperuniform scaling given in (5). Since  $\alpha$  is negative, the number variance grows faster than the window volume, i.e., faster than  $R^d$ . Up to a trivial constant in the leading-order term in the asymptotic expansion of the number variance given by (A1), one can view a “typical” nonhyperuniform system in which  $S(0)$  is bounded as one in which  $\alpha = 0^+$  (approaches zero from above), even if  $S(\mathbf{k})$  is not described by a power-law form in the zero-wavenumber limit. This enables one to conclude that  $A_N(R)$  converges to a constant in the limit  $R \rightarrow \infty$ , thus yielding the  $R^d$  scaling behavior for  $\sigma^2(R)$  in (5).

### Appendix B: Evaluation of the coefficients $A$ and $B$ for a Super-Poissonian Point Pattern

Any nonhyperuniform point process for which  $S(0) > 1$  has a large- $R$  asymptotic number variance  $\sigma^2(R)$  that is larger than that for a Poisson point process [ $S(0) = 1$ ] with the same mean  $\langle N(R) \rangle$  is called *super-Poissonian* [56]. We evaluate the volume and surface-area coefficients  $A$  and  $B$  for a specific model of a super-Poissonian point process, namely, the *Poisson cluster process*, which is characterized by strong clustering of the points with a large but finite value of  $S(0)$ , and hence is far from being hyperuniform. The higher-order moments of the number fluctuations as well as the corresponding probability distribution for this model were recently studied [56]. The construction of the cluster process starts from a homogeneous Poisson point process of intensity  $\rho_p$  [79]. Each point of the Poisson point process is the center of a cluster of points. The number of points in each cluster is independent and follows a Poisson distribution with mean value  $c$ . Following Ref. [56], we consider here the

special case in which the positions of the points relative to the center of the cluster follow an isotropic Gaussian distribution with standard deviation  $r_0$ , which can be regarded to be the characteristic length scale of a single cluster. In the infinite-volume limit, the structure factor for any  $d$  is exactly given by [56]

$$S(k) = 1 + ce^{-k^2 r_0^2}. \quad (\text{B1})$$

It immediately follows from this formula and (21) that  $S(0) = A = 1 + c$ . Using the Fourier representation of the surface-area coefficient (44) and relation (B1), we find that  $B$ , for any  $d$ , is exactly given by

$$B = -\frac{c r_0 d}{\sqrt{\pi}}. \quad (\text{B2})$$

Remarkably, this model provides an example of a surface-area coefficient that is negative (when  $c$  is positive), which heretofore has not been identified. Since the surface-area coefficient  $B$  is derived from the large- $R$  asymptotic expansion (20) of the number variance  $\sigma^2(R)$ , which must be positive, the length scale  $r_0$  in (B2), as any characteristic length scale, must be much smaller than the window radius  $R$ .

### Appendix C: Sum Rules and Large- $k$ Asymptotic Behaviors of $S(k)$ for Sphere Packings

Here we present sum rules as well as the exact large- $k$  asymptotic behaviors of the structure factors of certain general packings of identical spheres that apply in any space dimension  $d$ .

For a large class of packings of identical spheres of diameter  $D$ , the following sum rule applies inside the hard core:

$$\frac{r}{(2\pi r)^{\frac{d}{2}}} \int_0^\infty k^{d/2} \tilde{h}(k) J_{(d/2)-1}(kr) dk = -1 \quad \text{for } r < D. \quad (\text{C1})$$

This sum rule follows from the fact that  $h(\mathbf{r}) = -1$  for  $r < D$  and use of (29). It is valid provided that the volume integral of  $\tilde{h}(\mathbf{k})$  over all reciprocal space is bounded. In the special case of  $r = 0$ , (C1) yields

$$\frac{d}{2^d \pi^{d/2} \Gamma(1 + d/2)} \int_0^\infty k^{d-1} \tilde{h}(k) dk = -1. \quad (\text{C2})$$

Such exact sum rules can be utilized to check the accuracy of the determination of  $S(k)$  of sphere packings via experimental or numerical methods.

The Fourier transform of the indicator function  $m(r; a) = \Theta(a - r)$  for a  $d$ -dimensional sphere of radius  $a$  is given by

$$\begin{aligned} \tilde{m}(k; a) &= \frac{(2\pi)^{d/2}}{k^{(d/2)-1}} \int_0^a r^{d/2} J_{(d/2)-1}(kr) dr \\ &= \left(\frac{2\pi}{ka}\right)^{d/2} a^d J_{d/2}(ka). \end{aligned} \quad (\text{C3})$$

For large  $k$ , this Fourier transform is given by

$$\tilde{m}(k; a) \sim R^d (2\pi)^{d/2} \sqrt{2/\pi} \frac{\cos[ka - (d+1)/4]}{(ka)^{(d+1)/2}} + \mathcal{O}\left(\frac{1}{(ka)^{(d+3)/2}}\right) \quad (\text{C4})$$

For any packing of spheres of diameter  $D$ ,  $h(r) = -m(r; D)$  for  $r < D$ . Let us assume that the contact-value of the pair correlation function, denoted by  $g_2(D^+)$ , is bounded, i.e., the jump discontinuity at contact is finite. Using the result (C4) for such a packing, we can relate the large- $k$  behavior of the structure factor in terms of  $g_2(D^+)$ :

$$\begin{aligned} S(k) \sim 1 - \phi g_2(D^+) 2^{3d/2} \Gamma(1 + d/2) \sqrt{2/\pi} \frac{\cos[kD - (d+1)/4]}{(kD)^{(d+1)/2}} \\ + \mathcal{O}\left(\frac{1}{(kD)^{(d+3)/2}}\right) \quad (kD \rightarrow \infty). \end{aligned} \quad (\text{C5})$$

For  $d = 1, 2$  and  $3$ , the corresponding asymptotic behaviors are explicitly given respectively by

$$S(k) \sim 1 - 2\phi g_2(D^+) \frac{\sin(kD)}{kD} + \mathcal{O}\left(\frac{1}{(kD)^2}\right) \quad (d = 1), \quad (\text{C6})$$

$$S(k) \sim 1 - 8\sqrt{2/\pi} \phi g_2(D^+) \frac{\cos(kD + \pi/4)}{(kD)^{3/2}} + \mathcal{O}\left(\frac{1}{(kD)^{5/2}}\right) \quad (d = 2) \quad (\text{C7})$$

and

$$S(k) \sim 1 + 24\phi g_2(D^+) \frac{\cos(kD)}{(kD)^2} + \mathcal{O}\left(\frac{1}{(kD)^3}\right) \quad (d = 3). \quad (\text{C8})$$

We see that the rate of decay of  $S(k)$  increases as  $d$  increases.

By contrast, if the sphere packing is disordered at a jammed state with average contact number per particle of  $Z$ , then the jamming-contact condition is described by

$$g_2(r) \sim \frac{Z}{\rho s_1(1) D^{d-1}} \delta(r - D), \quad (\text{C9})$$

where  $s_1(1) = dv_1(1)$  is the  $d$ -dimensional surface area of a sphere of unit radius. Thus, we see for such jammed packings, the large- $k$  behavior of the structure factor is given by

$$\begin{aligned} S(k) \sim 1 + \frac{2^{d/2} \Gamma(1 + d/2) Z}{d} \frac{J_{d/2-1}(kD)}{(kD)^{d/2-1}} \\ + \mathcal{O}\left(\frac{1}{(kD)^{(d+1)/2}}\right) \quad (kD \rightarrow \infty). \end{aligned} \quad (\text{C10})$$

For  $d = 1, 2$  and  $3$ , the corresponding asymptotic behaviors are explicitly given respectively by

$$S(k) \sim 1 + Z \cos(kD) + \mathcal{O}\left(\frac{1}{(kD)}\right) \quad (d = 1) \quad (\text{C11})$$

$$S(k) \sim 1 + Z J_0(kD) + \mathcal{O}\left(\frac{1}{(kD)^{3/2}}\right) \quad (d = 2) \quad (\text{C12})$$



$$S(k) \sim 1 + Z \frac{\sin(kD)}{kD} + \mathcal{O}\left(\frac{1}{(kD)^2}\right) \quad (d = 3). \quad (\text{C13})$$

Again, we see that the rate of decay of  $S(k)$  increases as  $d$  increases, but less rapidly than in unjammed packings at the same dimension in which the jump discontinuity in  $g_2(r)$  at contact is finite.

## ACKNOWLEDGMENTS

The author is grateful to Jaek Kim, Michael Klatt, Charles Maher, Murray Skolnick and Haina Wang for

their careful reading of the manuscript. This work was supported by the National Science Foundation under Award No. DGE-2039656.

\* Email: torquato@princeton.edu

- 
- [1] S. Torquato and F. H. Stillinger, “Local density fluctuations, hyperuniform systems, and order metrics,” *Phys. Rev. E* **68**, 041113 (2003).
- [2] S. Torquato, “Hyperuniform states of matter,” *Physics Reports* **745**, 1–95 (2018).
- [3] J. P. Hansen and I. R. McDonald, *Theory of Simple Liquids*, 4th ed. (Academic Press, New York, 2013).
- [4] M. Florescu, S. Torquato, and P. J. Steinhardt, “Designer disordered materials with large complete photonic band gaps,” *Proc. Nat. Acad. Sci.* **106**, 20658–20663 (2009).
- [5] C. De Rosa, F. Auriemma, C. Diletto, R. Di Girolamo, A. Malafrente, P. Morvillo, G. Zito, G. Rusciano, G. Pesce, and A. Sasso, “Toward hyperuniform disordered plasmonic nanostructures for reproducible surface-enhanced Raman spectroscopy,” *Phys. Chem. Chem. Phys.* **17**, 8061–8069 (2015).
- [6] O. Leseur, R. Pierrat, and R. Carminati, “High-density hyperuniform materials can be transparent,” *Optica* **3**, 763–767 (2016).
- [7] T. Ma, H. Guerboukha, M. Girard, A. D. Squires, R. A. Lewis, and M. Skorobogatiy, “3D printed hollow-core terahertz optical waveguides with hyperuniform disordered dielectric reflectors,” *Adv. Optical Mater.* **4**, 2085–2094 (2016).
- [8] G. Zhang, F. H. Stillinger, and S. Torquato, “Transport, geometrical and topological properties of stealthy disordered hyperuniform two-phase systems,” *J. Chem. Phys.* **145**, 244109 (2016).
- [9] G. Gkantounis, T. Amoah, and M. Florescu, “Hyperuniform disordered phononic structures,” *Phys. Rev. B* **95**, 094120 (2017).
- [10] L. S. Froufe-Pérez, M. Engel, J. José Sáenz, and F. Scheffold, “Transport Phase Diagram and Anderson Localization in Hyperuniform Disordered Photonic Materials,” *Proc. Nat. Acad. Sci.* **114**, 9570–9574 (2017).
- [11] D. Chen and S. Torquato, “Designing disordered hyperuniform two-phase materials with novel physical properties,” *Acta Materialia* **142**, 152–161 (2018).
- [12] H. Zhang, W. Wu, and Y. Hao, “Luneburg lens from hyperuniform disordered composite materials,” in *2018 IEEE International Symposium on Antennas and Propagation & USNC/URSI National Radio Science Meeting* (2018) pp. 2281–2282.
- [13] S. Gorsky, W. A. Britton, Y. Chen, J. Montaner, A. Lenef, M. Raukas, and L. Dal Negro, “Engineered hyperuniformity for directional light extraction,” *APL Photonics* **4**, 110801 (2019).
- [14] A. Sheremet, R. Pierrat, and R. Carminati, “Absorption of scalar waves in correlated disordered media and its maximization using stealth hyperuniformity,” *Phys. Rev. A* **101**, 053829 (2020).
- [15] J. Kim and S. Torquato, “Multifunctional composites for elastic and electromagnetic wave propagation,” *Proc. Nat. Acad. Sci.* **117**, 8764–8774 (2020).
- [16] S. Yu, C.-W. Qiu, Y. Chong, S. Torquato, and N. Park, “Engineered disorder in photonics,” *Nature Rev. Mater.* **6**, 226–243 (2021).
- [17] C. E. Zachary and S. Torquato, “Hyperuniformity in point patterns and two-phase heterogeneous media,” *J. Stat. Mech.: Theory & Exp.* **2009**, P12015 (2009).
- [18] C. Lin, P. J. Steinhardt, and S. Torquato, “Hyperuniformity variation with quasicrystal local isomorphism class,” *J. Phys.: Cond. Matter* **29**, 204003 (2017).
- [19] E. C. Oğuz, J. E. S. Socolar, P. J. Steinhardt, and S. Torquato, “Hyperuniformity of quasicrystals,” *Phys. Rev. B* **95**, 054119 (2017).
- [20] A. Gabrielli, “Point processes and stochastic displacement fields,” *Phys. Rev. E* **70**, 066131 (2004).
- [21] A. Gabrielli and S. Torquato, “Voronoi and void statistics for superhomogeneous point processes,” *Phys. Rev. E* **70**, 041105 (2004).
- [22] A. Gabrielli, M. Joyce, and S. Torquato, “Tilings of space and superhomogeneous point processes,” *Phys. Rev. E* **77**, 031125 (2008).
- [23] J. Kim and S. Torquato, “Effect of imperfections on the hyperuniformity of many-body systems,” *Phys. Rev. B* **97**, 054105 (2018).
- [24] O. U. Uche, F. H. Stillinger, and S. Torquato, “Constraints on collective density variables: Two dimensions,” *Phys. Rev. E* **70**, 046122 (2004).
- [25] S. Torquato, G. Zhang, and F. H. Stillinger, “Ensemble theory for stealthy hyperuniform disordered ground states,” *Phys. Rev. X* **5**, 021020 (2015).
- [26] G. Zhang, F. H. Stillinger, and S. Torquato, “The perfect glass paradigm: Disordered hyperuniform glasses down to absolute zero,” *Sci. Rep.* **6**, 36963 (2016).
- [27] Q.-L. Lei and R. Ni, “Hydrodynamics of random-organizing hyperuniform fluids,” *Proc. Nat. Acad. Sci.*

- 116**, 22983–22989 (2019).
- [28] S. Torquato, G. Zhang, and M. de Courcy-Ireland, “Hidden multiscale order in the primes,” *J. Phys. A: Math. & Theoretical* **52**, 135002 (2019).
- [29] A. Donev, F. H. Stillinger, and S. Torquato, “Unexpected density fluctuations in disordered jammed hard-sphere packings,” *Phys. Rev. Lett.* **95**, 090604 (2005).
- [30] C. E. Zachary, Y. Jiao, and S. Torquato, “Hyperuniform long-range correlations are a signature of disordered jammed hard-particle packings,” *Phys. Rev. Lett.* **106**, 178001 (2011).
- [31] Y. Jiao and S. Torquato, “Maximally random jammed packings of Platonic solids: Hyperuniform long-range correlations and isostaticity,” *Phys. Rev. E* **84**, 041309 (2011).
- [32] S. Atkinson, G. Zhang, A. B. Hopkins, and S. Torquato, “Critical slowing down and hyperuniformity on approach to jamming,” *Phys. Rev. E* **94**, 012902 (2016).
- [33] R. P. Feynman and M. Cohen, “Energy spectrum of the excitations in liquid helium,” *Phys. Rev.* **102**, 1189–1204 (1956).
- [34] L. Reatto and G. V. Chester, “Phonons and the properties of a Bose system,” *Phys. Rev.* **155**, 88–100 (1967).
- [35] S. Torquato, A. Scardicchio, and C. E. Zachary, “Point processes in arbitrary dimension from Fermionic gases, random matrix theory, and number theory,” *J. Stat. Mech.: Theory Exp.* **2008**, P11019 (2008).
- [36] C. E. Zachary and S. Torquato, “Anomalous local coordination, density fluctuations, and void statistics in disordered hyperuniform many-particle ground states,” *Phys. Rev. E* **83**, 051133 (2011).
- [37] D. Hexner and D. Levine, “Hyperuniformity of critical absorbing states,” *Phys. Rev. Lett.* **114**, 110602 (2015).
- [38] B. Widom, “Equation of state in the neighborhood of the critical point,” *J. Chem. Phys.* **43**, 3898–3905 (1965).
- [39] L. P. Kadanoff, “Scaling laws for Ising models near  $T_c$ ,” *Physics* **2**, 263–272 (1966).
- [40] M. E. Fisher, “The theory of equilibrium critical phenomena,” *Rep. Prog. Phys.* **30**, 615 (1967).
- [41] K. G. Wilson and J. Kogut, “The renormalization group and the  $\epsilon$  expansion,” *Phys. Rep.* **12**, 75–199 (1974).
- [42] J. J. Binney, N. J. Dowrick, A. J. Fisher, and M. E. J. Newman, *The Theory of Critical Phenomena: An Introduction to the Renormalization Group* (Oxford University Press, Oxford, England, 1992).
- [43] E. C. Oğuz, J. E. S. Socolar, P. J. Steinhardt, and S. Torquato, “Hyperuniformity and anti-hyperuniformity in one-dimensional substitution tilings,” *Acta Cryst. Section A: Foundations & Advances* **75** (2019).
- [44] R. Dreyfus, Y. Xu, T. Still, L. A. Hough, A. G. Yodh, and S. Torquato, “Diagnosing hyperuniformity in two-dimensional, disordered, jammed packings of soft spheres,” *Phys. Rev. E* **91**, 012302 (2015).
- [45] L. S. Ornstein and F. Zernike, “Accidental deviations of density and opalescence at the critical point of a single substance,” *Proc. Akad. Sci. (Amsterdam)* **17**, 793–806 (1914).
- [46] A. B. Hopkins, F. H. Stillinger, and S. Torquato, “Nonequilibrium static diverging length scales on approaching a prototypical model glassy state,” *Phys. Rev. E* **86**, 021505 (2012).
- [47] S. Torquato, T. M. Truskett, and P. G. Debenedetti, “Is random close packing of spheres well defined?” *Phys. Rev. Lett.* **84**, 2064–2067 (2000).
- [48] É. Marcotte, F. H. Stillinger, and S. Torquato, “Nonequilibrium static growing length scales in supercooled liquids on approaching the glass transition,” *J. Chem. Phys.* **138**, 12A508 (2013).
- [49] A. Chremos and J. F. Douglas, “Particle localization and hyperuniformity of polymer-grafted nanoparticle materials,” *Annalen der Physik* **529** (2017).
- [50] A. Chremos and J. F. Douglas, “Hidden hyperuniformity in soft polymeric materials,” *Phys. Rev. Lett.* **121**, 258002 (2018).
- [51] F. Martelli, S. Torquato, N. Giovambattista, and R. Car, “Large-scale structure and hyperuniformity of amorphous ices,” *Phys. Rev. Lett.* **119**, 136002 (2017).
- [52] Y. Zhou, B. Mei, and K. S. Schweizer, “Integral equation theory of thermodynamics, pair structure, and growing static length scale in metastable hard sphere and weeks-chandler-andersen fluids,” *Phys. Rev. E* **101**, 042121 (2020).
- [53] M. A. Klatt, J. Lovrić, D. Chen, S. C. Kapfer, F. M. Schaller, P. W. A. Schönhofer, B. S. Gardiner, A.-S. Smith, G. E. Schröder-Turk, and S. Torquato, “Universal hidden order in amorphous cellular geometries,” *Nature Comm.* **10**, 811 (2019).
- [54] T. M. Hain, M. A. Klatt, and G. E. Schröder-Turk, “Low-temperature statistical mechanics of the Quantizer problem: Fast quenching and equilibrium cooling of the three-dimensional Voronoi liquid,” *J. Chem. Phys.* **153**, 234505 (2020).
- [55] G. Zhang and S. Torquato, “Realizable hyperuniform and nonhyperuniform particle configurations with targeted spectral functions via effective pair interactions,” *Phys. Rev. E* **101**, 032124 (2020).
- [56] S. Torquato, J. Kim, and M. A. Klatt, “Local number fluctuations in hyperuniform and nonhyperuniform systems: Higher-order moments and distribution functions,” *Phys. Rev. X* (2021).
- [57] S. Torquato, *Random Heterogeneous Materials: Microstructure and Macroscopic Properties* (Springer-Verlag, New York, 2002).
- [58] B. J. Alder and T. E. Wainwright, “Phase transition for a hard sphere system,” *J. Chem. Phys.* **27**, 1208–1209 (1957).
- [59] D. Frenkel, “Entropy-driven phase transitions,” *Physica A* **263**, 26–38 (1999).
- [60] S. C. Mau and D. A. Huse, “Stacking entropy of hard-sphere crystals,” *Phys. Rev. E* **59**, 4396–4401 (1999).
- [61] S. Torquato and F. H. Stillinger, “Jammed hard-particle packings: From Kepler to Bernal and beyond,” *Rev. Mod. Phys.* **82**, 2633 (2010).
- [62] S. Torquato and F. H. Stillinger, “Multiplicity of generation, selection, and classification procedures for jammed hard-particle packings,” *J. Phys. Chem. B* **105**, 11849–11853 (2001).
- [63] A. Donev, S. Torquato, F. H. Stillinger, and R. Connelly, “A linear programming algorithm to test for jamming in hard-sphere packings,” *J. Comput. Phys.* **197**, 139–166 (2004).
- [64] S. Torquato and F. H. Stillinger, “Toward the jamming threshold of sphere packings: Tunneled crystals,” *J. Appl. Phys.* **102**, 093511 (2007), Erratum, **103**, 129902 (2008).
- [65] S. Torquato, A. Donev, and F. H. Stillinger, “Breakdown of elasticity theory for jammed hard-particle packings: Conical nonlinear constitutive theory,” *Int. J. Solids*

- Structures **40**, 7143–7153 (2003).
- [66] Z. W. Salsburg and W. W. Wood, “Equation of state of classical hard spheres at high density,” *J. Chem. Phys.* **37**, 798–1025 (1962).
- [67] F. H. Stillinger and Z. W. Salsburg, “Limiting polytope geometry for rigid rods, disks, and spheres,” *J. Stat. Phys.* **1**, 179–225 (1969).
- [68] A. Donev, S. Torquato, and F. H. Stillinger, “Pair correlation function characteristics of nearly jammed disordered and ordered hard-sphere packings,” *Phys. Rev. E* **71**, 011105: 1–14 (2005).
- [69] G. Parisi and F. Zamponi, “Mean field theory of hard sphere glasses and jamming,” *Rev. Mod. Phys.* **82**, 789–845 (2010).
- [70] J. Percus, “Pair distribution function in classical statistical mechanics,” in *The Equilibrium Theory of Classical Fluids*, edited by H. L. Frisch and J. L. Lebowitz (Benjamin, 1964).
- [71] L. Tonks, “The complete equation of state of one, two and three-dimensional gases of hard elastic spheres,” *Phys. Rev.* **50**, 955–963 (1936).
- [72] J. Kim and S. Torquato, “Effect of window shape on the detection of hyperuniformity via the local number variance,” *J. Stat. Mech.: Th. and Exper.* **2017**, 013402 (2017).
- [73] S. Torquato and F. H. Stillinger, “Controlling the short-range order and packing densities of many-particle systems,” *J. Phys. Chem. B* **106**, 8354–8359 (2002), Erratum **106**, 11406 (2002).
- [74] H. Cohn and N. Elkies, “New upper bounds on sphere packings I,” *Annals Math.* **157**, 689–714 (2003).
- [75] S. Torquato and F. H. Stillinger, “New conjectural lower bounds on the optimal density of sphere packings,” *Experimental Math.* **15**, 307–331 (2006).
- [76] O. U. Uche, F. H. Stillinger, and S. Torquato, “On the realizability of pair correlation functions,” *Physica A* **360**, 21–36 (2006).
- [77] K. Ball, “A lower bound for the optimal density of lattice packings,” *Int. Math. Res. Notices* **68**, 217–221 (1992).
- [78] R. D. Batten, F. H. Stillinger, and S. Torquato, “Classical disordered ground states: Super-ideal gases, and stealth and equi-luminous materials,” *J. Appl. Phys.* **104**, 033504 (2008).
- [79] G. Last and M. Penrose, *Lectures on the Poisson Process*, Institute of Mathematical Statistics Textbooks (Cambridge University Press, Cambridge, United Kingdom, 2017).